

10238
NACA TN 3871

TECH LIBRARY KAFB, NM
0067084

NATIONAL ADVISORY COMMITTEE FOR AERONAUTICS

TECHNICAL NOTE 3871

AN INVESTIGATION AT SUBSONIC SPEEDS OF SEVERAL MODIFICATIONS
TO THE LEADING-EDGE REGION OF THE NACA 64A010 AIRFOIL
SECTION DESIGNED TO INCREASE MAXIMUM LIFT

By Ralph L. Maki and Lynn W. Hunton

Ames Aeronautical Laboratory
Moffett Field, Calif.

AFMDC Technical Library
AFL 2811



Washington
December 1956

AFMDC
TECHNICAL LIBRARY
AFL 2811



0067084

NATIONAL ADVISORY COMMITTEE FOR AERONAUTICS

TECHNICAL NOTE 3871

AN INVESTIGATION AT SUBSONIC SPEEDS OF SEVERAL MODIFICATIONS
TO THE LEADING-EDGE REGION OF THE NACA 64A010 AIRFOIL
SECTION DESIGNED TO INCREASE MAXIMUM LIFT

By Ralph L. Maki and Lynn W. Hunton

SUMMARY

Three modifications to the leading-edge region of the NACA 64A010 airfoil section were designed and tested two-dimensionally at both low and high subsonic speeds. The modifications increased the low-speed maximum lift coefficient of the symmetrical reference section by as much as 0.58, largely by increasing the angle of attack at which stall occurred. A single-criterion design procedure for estimating the incremental maximum lift due to an arbitrary modification, based on control of the theoretical pressure peak, was unsatisfactory.

Tests at high speeds showed that the maximum-lift increments provided by the leading-edge changes were reduced by compressibility effects, and vanished at about a Mach number of 0.65. The high-speed drag characteristics of a modified section with 1.1-percent-chord nose radius and camber over the forward 15-percent chord were somewhat improved over those of the NACA 64A010 section.

INTRODUCTION

To maintain attached flow over given airfoils to higher angles of attack, a method frequently used has been one which entails modification of the leading-edge region by introduction of forward camber and/or an increase of leading-edge radius (see refs. 1 to 7). Tests of such changes were limited to arbitrary designs. To furnish additional data useful both for low-speed design and high-speed evaluation, three related contour changes for the NACA 64A010 airfoil section were tested two-dimensionally at both low and high subsonic speeds. One of the modified airfoils was so designed as to have the same nose radius and type of camber as a standard designated section, the NACA 13010.

This report presents the test results and compares airfoils having forward and distributed types of camber.

NOTATION

c	chord
c_d	section drag coefficient
c_l	section lift coefficient
c_{l_i}	design section lift coefficient
c_m	section pitching-moment coefficient about $\frac{c}{4}$
c_n	section normal-force coefficient
C_p	local pressure coefficient, $\frac{p_l - p}{q}$
M	Mach number
M_d	drag-divergence Mach number, defined as the Mach number at which $\frac{dc_d}{dM} = 0.1$
p	free-stream static pressure
p_l	local static pressure
q	free-stream dynamic pressure
R	Reynolds number, $\frac{Vc}{\nu}$
r	leading-edge radius in percent of chord
V	free-stream velocity
v	local velocity on the symmetrical section
Δv	increment of local velocity induced by section camber
x	distance along airfoil chord, measured from the leading edge of the uncambered section
y	height above airfoil chord
α_o	section angle of attack, measured with respect to the chord line
α_B	section angle of attack, measured with respect to chord line of the unmodified section

ν kinematic viscosity

Subscripts

max maximum

min minimum

o conditions at zero section lift, except as otherwise defined above

u uncorrected

MODELS AND TESTS

Airfoils

Three related airfoil profiles were designed for this study. The profiles were formed by modifying the forward 20-percent chord of the NACA 64A010 section to incorporate camber and increases in nose radius. Selection of these nose modifications was guided by a simple design criterion based on control of the theoretical leading-edge velocity peak. This design criterion will be discussed later in the report.

One of the nose modifications (airfoil 2 in the table below) was designed to have the same leading-edge radius and similar camber distribution as a standard designated section, the NACA 13010. The other two sections differed either in leading-edge radius or type of camber line as shown in the table.

Airfoil designation	Leading-edge radius, percent chord	Leading-edge droop, percent chord	Similar NACA camber ¹	c_{l_i}
1	1.10	1.12	210	0.22
2	1.10	1.23	130	.15
3	1.50	1.23	130	.18

¹Similar as to chordwise distribution of camber, but with c_{l_i} shown in last column.

Profiles of the airfoils are shown in figure 1, and the coordinates are given in table I. Theoretical loadings and pressure distributions computed by the airfoil theories of references 8 and 9 are compared with those for the NACA 64A010 section in figures 2 and 3.

Low-Speed Tests

The low-speed tests were conducted in the Ames 7- by 10-foot wind tunnel number 1. The 5-foot-chord model of the NACA 64A010 section spanned the 7-foot height of the tunnel. Six-foot-diameter end plates attached to the model were flush with the tunnel walls, thus forming part of the floor and ceiling of the test section. The forward 20-percent chord of the model was removable for installation of the modified leading edges. The aft 25-percent chord was removable for tests with or without double-slotted flaps. For tests with zero flap deflection, the main flap of the double-slotted flaps formed the rear portion of the model; surfaces were sealed and smooth for these tests. For tests with double-slotted flaps deflected, the 0.075c foreflap was deflected 30° and the 0.25c main flap was deflected 55° . Flush pressure orifices were provided along the mid-span sections of the models.

Measurements of lift and pitching moment were made with the wind-tunnel balance system. Tunnel-wall corrections computed by the method of reference 10 were applied to the data as follows:

$$\alpha_s \text{ or } \alpha_o = \alpha_u + 0.47 c_{l_u} + 1.89 c_{m_u}$$

$$c_l = 0.930 c_{l_u}$$

$$c_m = 0.982 c_{m_u} + 0.013 c_{l_u}$$

Tests were made at Reynolds numbers of 2.8, 4.0, and 5.8×10^6 with the Mach number varying approximately from 0.08 to 0.17.

High-Speed Tests

The high-speed tests were conducted in the Ames 1- by 3-1/2-foot wind tunnel. Six-inch-chord models of the NACA 64A010 airfoil section and the modified sections were constructed of aluminum alloy. The models spanned the 1-foot dimension of the test section. Sponge-rubber gaskets were compressed between the model ends and the tunnel walls to prevent end leakage.

Lift, drag, and pitching moment were measured both at constant angle of attack while varying Mach number for all models and at constant Mach number while varying angle of attack for the modified airfoils. The Mach numbers ranged from 0.3 to about 0.9; the range of angles of attack was sufficient to define maximum lift up to a Mach number of about 0.8. The Reynolds numbers varied approximately from 1×10^6 at a Mach number of 0.3 to 2×10^6 at the highest test Mach numbers.

Lift and pitching moment were determined from measurements of the pressure reactions on the tunnel walls of the forces on the airfoils. Drag was determined from wake-survey measurements made with a rake of total-head tubes.

RESULTS AND DISCUSSION

Low Speed

Characteristics of the modified airfoils.- The basic lift and pitching-moment characteristics obtained from the low-speed force tests are presented in figures 4 and 5. Drag-force measurements obtained in the low-speed tests have not been presented since the results were found erroneous, apparently, due to drag and interference effects of the model end plates. However, the end plates apparently caused little effect on the over-all lift and moment results since checks of these data made with the pressure measurements revealed average differences of the order of only 1/2 percent.

Despite the variation in camber for the three airfoils, no particularly significant differences in the lift and moment characteristics can be detected in figure 4 aside from the obvious variation in $c_{l_{max}}$. All sections show virtually no lift or moment at zero angle of attack. In interpreting these data, it must be remembered that the line used in referencing α_s is the chord line of the unmodified section. This introduces a positive displacement of the lift curves of about 0.7° for all three modified sections as compared with the usual referencing system. At the highest test Reynolds number, the maximum lift peak for airfoils 1 and 2 can be seen to become more rounded than at the lower Reynolds numbers.

The stall development on the modified airfoils is illustrated in figure 6 with selected pressure distributions from 4.0 million Reynolds number data. Evidence of turbulent separation appears in the figures at the trailing edges of all three airfoils at $c_{l_{max}}$. Scrutiny of all the pressure data, in fact, showed that turbulent separation appeared just prior to $c_{l_{max}}$. Turbulent separation appears in the pressure data as a rise in pressures (more negative) near the trailing edge.

In the case of airfoil 1, the complete pressure-distribution data showed that this separation spread forward with increasing angle of attack, and $C_{p_{min}}$ remained at an almost constant value, establishing a $c_{l_{max}}$ value; even 2° beyond $c_{l_{max}}$, however, a peak of considerable magnitude was found. In contrast, the maximum lift of airfoils 2 and 3 was established as a result of flow separation occurring near the leading edge which joined the already existing trailing-edge flow separation; in these cases the nose peak was markedly reduced at angles above that for $c_{l_{max}}$. The pressure data for other Reynolds numbers showed that in all cases the evidence of trailing-edge flow separation became more apparent with increase in Reynolds number, but did not alter the sequence of stall

progression. Stall on the symmetrical reference section was similar to that for airfoils 2 and 3 in that the flow separated suddenly from points near the leading edge and free-stream static pressure was not regained at the trailing edge (ref. 11). However, data for the symmetrical section showed no evidence of trailing-edge flow separation prior to stall as previously indicated for airfoils 2 and 3. No definite evidence of a leading-edge separation bubble could be detected in the pressure data for the modified airfoils as was found for the NACA 64A010.

Data for the three airfoils with flap deflected are given in figure 5 for Reynolds numbers of 4.0 and 5.8 million. This flap, being of the double-slotted type, produced very large increments in lift but at the expense of very large pitching moments. At the lower Reynolds number, the increments in $c_{l_{max}}$ between the three airfoils generally follow the pattern found for the modified sections without flaps. For some unaccountable reason, however, increasing the Reynolds number to 5.8 million caused a large deleterious effect on the $c_{l_{max}}$ of airfoil 3, having the larger leading-edge radius, while little change can be seen to have occurred in the characteristics of the other sections.

Comparisons of airfoils with forward and distributed camber.- Gains in maximum lift similar to those realized with the sections with forward camber can be achieved through the use of distributed camber. In the following evaluation, the characteristics of airfoils of the latter type are included for comparative purposes. Similar comparisons are made for high speeds later in the report.

A direct comparison of the modified leading-edge section with a symmetrical section and sections having distributed camber is shown in figure 7. In the comparison, only airfoil 2 has been considered because in the high-speed tests, as will be seen in a subsequent section of the report, this airfoil exhibited generally superior characteristics over the others of the group. The lift curve for airfoil 2 has been displaced by 0.7° to the left so that α_0 is based on the usual chord line drawn from nose to trailing edge. The airfoils with distributed camber used for the correlation are the NACA 64A310 and 0010 with a c_{l_1} of 0.3, both using the NACA $a = 1.0$ mean line. Data on the cambered four-digit-section are included since its leading-edge radius is the same as that of airfoil 2. The data are those at 3.7 million Reynolds number reported in reference 12 from tests in the same facility used for the present low-speed study. Data for the NACA 64A010 included in figure 7 are those given in reference 11 (4.1 million Reynolds number).

The loading introduced by concentrating the camber near the nose produces almost no incremental pitching moment such as is associated with the distributed form of camber. This result is apparent in figure 7(a) and stems from the distribution of loading due to camber shown in figure 2(b). The increase in $c_{l_{max}}$ provided by distributed camber on the

NACA 64A310, $a = 1.0$, section is approximately equal to its c_{l_i} . That provided by the airfoil 2 modification is considerably more than its c_{l_i} (0.15), presumably due to the increase in leading-edge radius. The difference in leading-edge radius is also believed to be the principal reason for the difference in $c_{l_{max}}$ of the NACA sections 64A310, $a = 1.0$, and 0010 with a c_{l_i} of 0.3.

Data comparing three types of sections with flaps deflected are presented in figure 7(b). Here the distributed camber section used is the NACA 65-210 airfoil (data from ref. 13); the double-slotted flap configuration is identical for all three sections (main flap deflected 55°). From a comparison of the data of figures 7(a) and 7(b), flaps retracted and extended, it may be seen that the modification provided about the same incremental change in $c_{l_{max}}$ with the flap extended as with it retracted. The large pitching moment associated with flaps is little affected by either the modified leading edge or the distributed type of camber.

High Speed

Characteristics of the modified airfoils.- Lift, drag, and pitching-moment results for the three modified sections are presented in figures 8 to 12 for Mach numbers ranging from 0.3 to about 0.9. In figures 13 and 14, direct comparisons are made of the three modified sections showing the variation of $c_{l_{max}}$ and c_d as a function of Mach number while in figure 15 the drag-divergence Mach numbers are compared.

At these higher speeds the incremental differences in $c_{l_{max}}$ between airfoils are greatly diminished over those found at low speed. Moreover, the magnitudes of $c_{l_{max}}$ of the modified airfoils at $M = 0.3$ are only about 2/3 the lower speed values (fig. 13). This is due to both the difference in test Reynolds number for the low- and high-speed studies (2.8 million and about 1.0 to 2.0 million, respectively) and the increase in Mach number. A portion of the data of reference 14 which clearly illustrates these effects for the NACA 64-210 section is included in figure 13.

Values of $c_{l_{max}}$ for the modified sections decrease with increasing Mach number above 0.3 whereas the unmodified section shows essentially no change. Consequently, the improvements in $c_{l_{max}}$ provided by the leading-edge modifications diminish with increases in Mach number and virtually disappear at a Mach number of the order of 0.65. It is to be noted that if these sections are applied to a swept wing, the relieving effects of sweepback will increase the Mach number at which the $c_{l_{max}}$ benefits provided by the nose modifications would be expected to vanish.

The comparisons of drag in figure 14(a) for the three modified airfoils on the whole show airfoil 2 to have the lowest drag at angles of attack above about 2° . The drag-divergence Mach number also is highest for this airfoil at high lift coefficients. Below about 0.2 lift coefficient the differences in M_d can be seen to be negligible (fig. 15).

Comparisons of airfoils with forward and distributed camber.- Figures 16 to 20 have been prepared to illustrate the high-speed characteristics of airfoil 2 as compared to those of the basic airfoil thickness form having distributed camber (NACA 64A310, $a = 1.0$ section) and having no camber (NACA 64A010 section). Data for these airfoils were taken from reference 15. Included are comparisons of $c_{l_{max}}$, c_d , M_d , c_l/c_d , and c_{m_0} . The deleterious effects of reduced Reynolds number and increasing Mach number to 0.3 on $c_{l_{max}}$ are nearly equal for both types of cambered airfoils (fig. 16). With increase in Mach number above 0.3, the $c_{l_{max}}$ of the modified airfoil continues to decrease while that for the NACA 64A310 remains fairly constant. Apparently, the type of variation of $c_{l_{max}}$ in this Mach number range is associated with the nose shape of the section, and is unaffected by a distributed type of camber. This same conclusion can be drawn from the data presented in reference 16 for a group of 15-percent-thick sections. In that paper, data for sections with nose radii almost as large as that of airfoil 3 and with distributed camber show an almost constant $c_{l_{max}}$ in the same Mach number range, whereas data for the NACA 23015 (forward camber) shows a decrease in $c_{l_{max}}$ with increase in M above 0.3 similar to the decrease noted for airfoils 1, 2, and 3. The data presented in reference 17 indicates that the relatively constant $c_{l_{max}}$ characteristic exists for sections with both the NACA $a = 0.4$ and $a = 1.0$ mean lines, and for values of c_{l_1} at least up to 0.4.

Figure 18 shows that the drag-divergence Mach number for airfoil 2 is higher than for the NACA 64A010 section at lift coefficients above about 0.3, but lower than the NACA 64A310 section above about 0.4 lift coefficient. From a lift-drag-ratio standpoint (fig. 19), the modified airfoil is superior to the symmetrical NACA 64A010 section at Mach numbers below about 0.7, but it does not match up to the lift-drag-ratio characteristics of the equivalent distributed-camber section. These c_l/c_d gains for the modified airfoil are, however, made without introduction of a zero-lift pitching-moment increment (fig. 20).

Comparison of Measured and Estimated Maximum Lift Values

An attempt was made to estimate the increments in low-speed $c_{l_{max}}$ over that of the NACA 64A010 reference section provided by the three modifications tested. A simple procedure, based on control of the

leading-edge velocity peak, was used. The method proved unsatisfactory, and reasons for its failure became apparent from analysis of the pressure-distribution data. Since the method is typical of those tried by many investigators, a brief review of the procedure and results is given below.

To select a design criterion by which to estimate $c_{l_{\max}}$, it was reasoned that maximum lift is controlled principally by the rate of rise of the leading-edge velocity peaks with lift coefficient. A reduction in this rate of rise by modification of the leading-edge region of an airfoil would imply an increase in $c_{l_{\max}}$. Assuming further the simple concept of a unique limit in the attainable value of the minimum pressure coefficient, one could then determine $c_{l_{\max}}$, at least for a given class of airfoil sections such as was considered here. (It was essentially this concept that was applied to the derivation of the NACA X-006 airfoil sections. See ref. 18.) Theoretical peak negative pressure coefficients at experimental values of $c_{l_{\max}}$ were determined for a large number of 10-percent-thick sections. A limiting theoretical minimum pressure coefficient was chosen as $C_{p_{\min}} = -10.5$ from a scrutiny of these data as an average limiting value. The increment of $c_{l_{\max}}$ estimated for an arbitrary modification was taken to be the difference in theoretical c_l between the modified and the unmodified sections when $C_{p_{\min}}$ for each attained the limit value of -10.5. The theories of references 8 and 9 were used. Comparisons of estimated and experimental $\Delta c_{l_{\max}}$ values for airfoils 1, 2, and 3 are given in the following table:

Airfoil	Estimated $\Delta c_{l_{\max}}$	Experimental $c_{l_{\max}}$ ($R = 4 \times 10^6$)	Experimental $\Delta c_{l_{\max}}$
NACA 64A010 ¹		1.07	
1	0.38	1.36	0.29
2	.32	1.44	.37
3	.42	1.65	.58

¹ $c_{l_{\max}}$ value for the NACA 64A010 section from the data of reference 11.

The estimated values of $\Delta c_{l_{\max}}$ are unsatisfactory for airfoils 1 and 3, differing by approximately 30 percent from the measured results. Comparisons at other Reynolds numbers are similar. Inspection of the experimental pressure data showed that limit $C_{p_{\min}}$ was not a single value for the modified sections as assumed, but varied from -9.5 to

beyond -13 . The value of $C_{p_{min}}$ occurred within the forward 1/2-percent chord, a region difficult to define by the usual airfoil theory procedures. Further examination of the pressure data revealed no method of improving the correlations with measured $c_{l_{max}}$ values. Thus it appears that prediction of $c_{l_{max}}$ for arbitrary profiles is beyond the reach of such a simple procedure.

CONCLUSIONS

Three modifications to the leading-edge region of the NACA 64A010 airfoil section were designed and tested two-dimensionally at both low and high subsonic speeds.

Tests at low speed showed that the leading-edge modifications were capable of increasing maximum lift coefficient of the 10-percent-thick section by as much as 0.58. Increases in lift were achieved largely by increases in the angle of attack at which stall occurred. The nose modifications introduced virtually no incremental pitching moment (such as is associated with sections with distributed forms of camber). A simple design procedure for estimating the incremental maximum lift due to an arbitrary modification, based on control of the theoretical minimum pressure, was unsatisfactory.

Tests at high speeds showed the increments in maximum lift provided by the leading-edge modifications were reduced by compressibility effects, and vanished at a Mach number of about 0.65. This is in contrast to the NACA 64A310 section (with a distributed form of camber) which provided an almost constant increment of maximum lift above that of the uncambered section up to high subsonic Mach numbers. The high-speed drag characteristics of a modified section with 1.1-percent-chord nose radius and camber over the forward 15-percent chord were somewhat improved over those of the unmodified NACA 64A010 section. Increasing the nose radius to 1.5-percent chord had deleterious effects on these characteristics.

Ames Aeronautical Laboratory
National Advisory Committee for Aeronautics
Moffett Field, Calif., Sept. 24, 1956

REFERENCES

1. James, Harry A., and Dew, Joseph K.: Effects of Double-Slotted Flaps and Leading-Edge Modifications on the Low-Speed Characteristics of a Large-Scale 45° Swept-Back Wing With and Without Camber and Twist. NACA RM A51D18, 1951.

2. Maki, Ralph L.: Full-Scale Wind-Tunnel Investigation of the Effects of Wing Modifications and Horizontal-Tail Location on the Low-Speed Static Longitudinal Characteristics of a 35° Swept-Wing Airplane. NACA RM A52B05, 1952.
3. Maki, Ralph L., and Embry, Ursel R.: Effects of High-Lift Devices and Horizontal-Tail Location on the Low-Speed Characteristics of a Large-Scale 45° Swept-Wing Airplane Configuration. NACA RM A54E10, 1954.
4. Maki, Ralph L.: The Use of Two-Dimensional Section Data to Estimate the Low-Speed Wing Lift Coefficient at Which Section Stall First Appears on a Swept Wing. NACA RM A51E15, 1951.
5. Kelly, John A.: Effects of Modifications to the Leading-Edge Region on the Stalling Characteristics of the NACA 63₁-012 Airfoil Section. NACA TN 2228, 1950.
6. Demele, Fred A., and Sutton, Fred B.: The Effects of Increasing the Leading-Edge Radius and Adding Forward Camber on the Aerodynamic Characteristics of a Wing With 35° of Sweepback. NACA RM A50K28a, 1951.
7. Anderson, Seth B., Matteson, Frederick H., and Van Dyke, Rudolph D., Jr.: A Flight Investigation of the Effect of Leading-Edge Camber on the Aerodynamic Characteristics of a Swept-Wing Airplane. NACA RM A52L16a, 1953.
8. Allen, H. Julian: General Theory of Airfoil Sections Having Arbitrary Shape or Pressure Distribution. NACA Rep. 833, 1945.
9. Graham, David: A Modification to Thin-Airfoil-Section Theory, Applicable to Arbitrary Airfoil Sections, to Account for the Effects of Thickness on the Lift Distribution. NACA TN 2298, 1951.
10. Allen, H. Julian, and Vincenti, Walter G.: Wall Interference in a Two-Dimensional-Flow Wind Tunnel With Consideration of the Effect of Compressibility. NACA Rep. 782, 1944.
11. Peterson, Robert F.: The Boundary Layer and Stalling Characteristics of the NACA 64A010 Airfoil Section. NACA TN 2235, 1950.
12. McCullough, George B., and Haire, William M.: Low-Speed Characteristics of Four Cambered, 10-Percent-Thick NACA Airfoil Sections. NACA TN 2177, 1950.
13. Cahill, Jones F.: Two-Dimensional Wind-Tunnel Investigation of Four Types of High-Lift Flap on an NACA 65-210 Airfoil Section. NACA TN 1191, 1947.

14. Racisz, Stanley F.: Effects of Independent Variations of Mach Number and Reynolds Number on the Maximum Lift Coefficients of Four NACA 6-Series Airfoil Sections. NACA TN 2824, 1952.
15. Summers, James L., and Treon, Stuart L.: The Effects of Amount and Type of Camber on the Variation With Mach Number of the Aerodynamic Characteristics of a 10-Percent-Thick NACA 64A-Series Airfoil Section. NACA TN 2096, 1950.
16. Graham, Donald J., Nitzberg, Gerald E., and Olson, Robert N.: A Systematic Investigation of Pressure Distributions at High Speeds Over Five Representative NACA Low-Drag and Conventional Airfoil Sections. NACA Rep. 832, 1945.
17. Stivers, Louis S., Jr.: Effects of Subsonic Mach Number on the Forces and Pressure Distributions on Four NACA 64A-Series Airfoil Sections at Angles of Attack as High as 28° . NACA TN 3162, 1954.
18. Loftin, Laurence K., and von Doenhoff, Albert E.: Exploratory Investigation at High and Low Subsonic Mach Numbers of Two Experimental 6-Percent-Thick Airfoil Sections Designed to Have High Maximum Lift Coefficients. NACA RM L51FO6, 1951.

TABLE I.- COORDINATES OF THE NACA 64A010 AND THE MODIFIED AIRFOIL SECTIONS
[Dimensions given in percent of chord]

x	NACA 64A010 y		Airfoil 1 y		Airfoil 2 y		Airfoil 3 y	
	Upper	Lower	Upper	Lower	Upper	Lower	Upper	Lower
0	0			-1.12		-1.23		-1.23
.25	---	---	0.355	---	-0.29	-1.75	-0.06	---
.50	.804	-0.804	.65	-1.625	.02	-2.00	.30	-2.15
.75	.969	-.969	.89	-1.71	.25	-2.165	.575	-2.35
1.00	---	---	1.09	-1.77	.45	-2.30	.805	-2.53
1.25	1.225	-1.225	1.265	-1.835	---	---	---	---
1.50	---	---	---	---	.80	-2.505	1.19	-2.795
2.00	---	---	1.705	-2.025	1.095	-2.67	1.51	-2.995
2.50	1.688	-1.688	1.935	-2.15	1.345	-2.79	1.78	-3.155
3.50	---	---	2.31	-2.395	1.76	-2.99	2.215	-3.395
5.00	2.327	-2.327	2.725	-2.735	2.265	-3.195	2.71	-3.62
7.50	2.805	-2.805	3.155	-3.15	2.875	-3.42	3.255	-3.80
10	3.199	-3.199	3.45	-3.45	3.305	-3.59	3.615	-3.90
12.50	---	---	---	---	3.655	-3.755	3.86	-3.99
15	3.813	-3.813	3.935	-3.935	3.94	-3.945	4.035	-4.07
17.50	---	---	---	---	4.125	-4.11	4.15	-4.155
20	4.272	-4.272	Applicable to airfoils 1, 2, and 3					
25	4.606	-4.606						
30	4.837	-4.837						
35	4.968	-4.968						
40	4.995	-4.995						
45	4.894	-4.894						
50	4.684	-4.684						
55	4.388	-4.388						
60	4.021	-4.021						
65	3.597	-3.597						
70	3.127	-3.127						
75	2.623	-2.623						
80	2.103	-2.103						
85	1.582	-1.582						
90	1.062	-1.062						
95	.541	-.541						
100	.021	-.021						
Leading-edge radius: 0.687			1.10; center at (0.992, -0.645)		1.10; center at (1.085, -1.045)		1.50; center at (1.480, -0.983)	

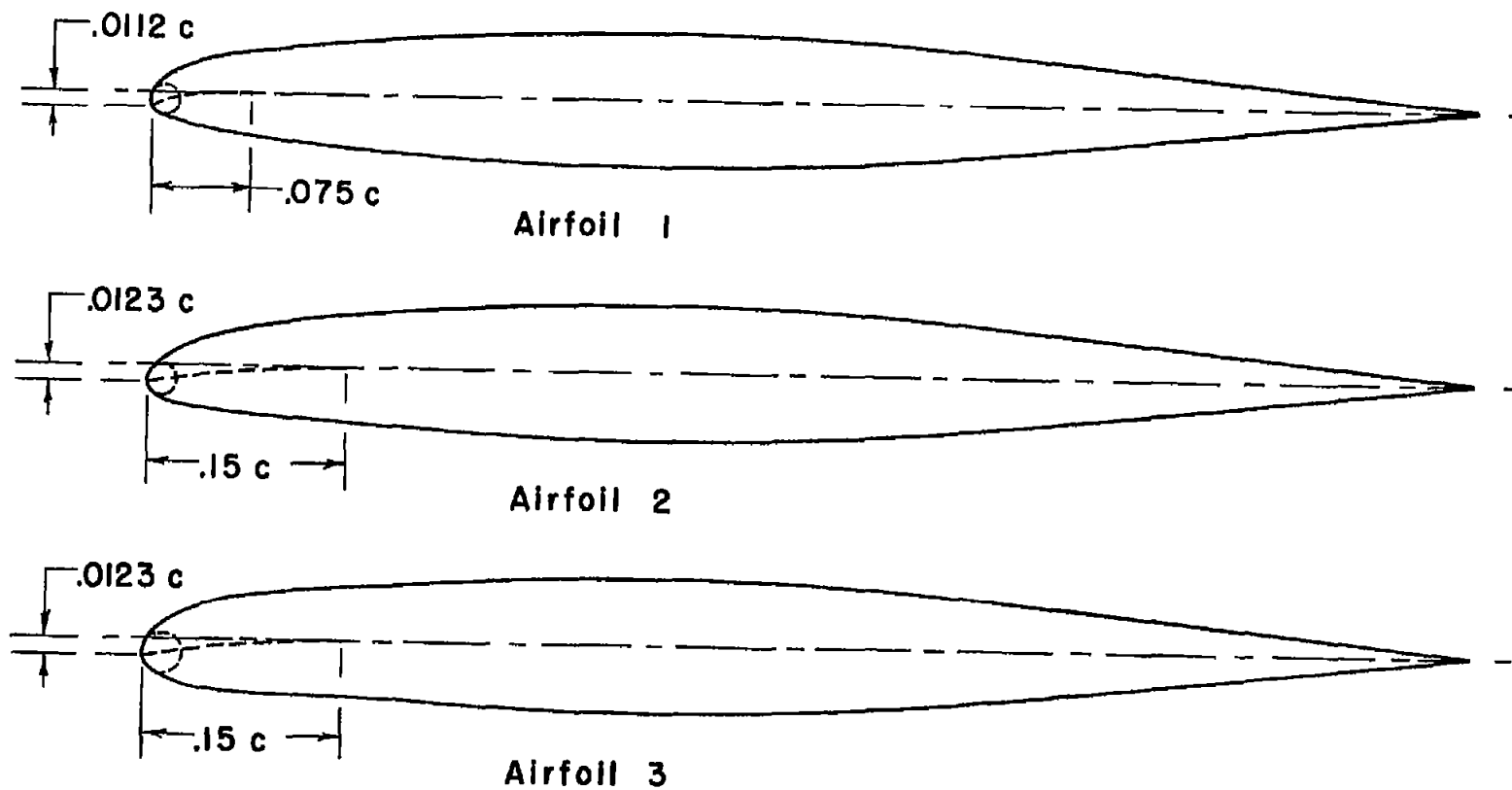
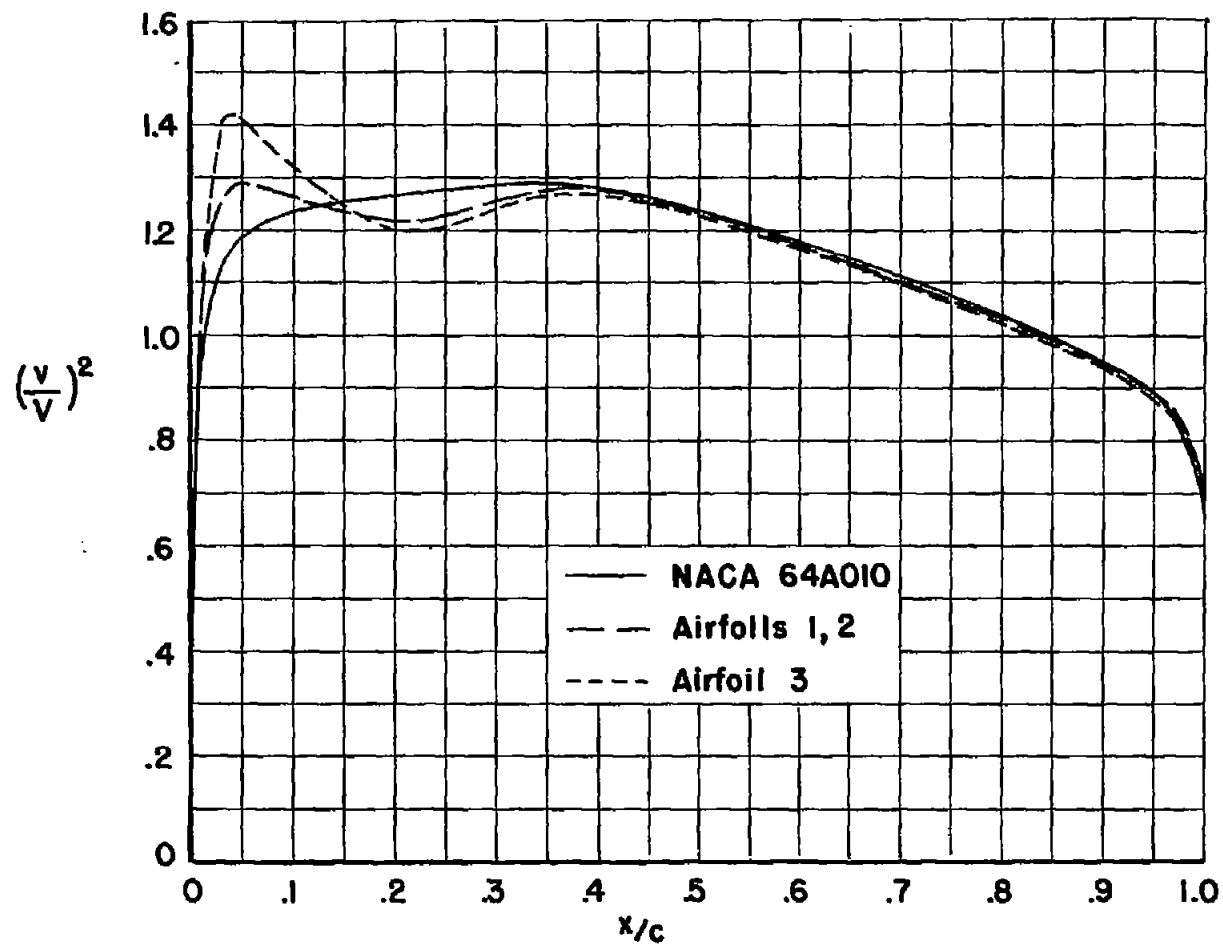
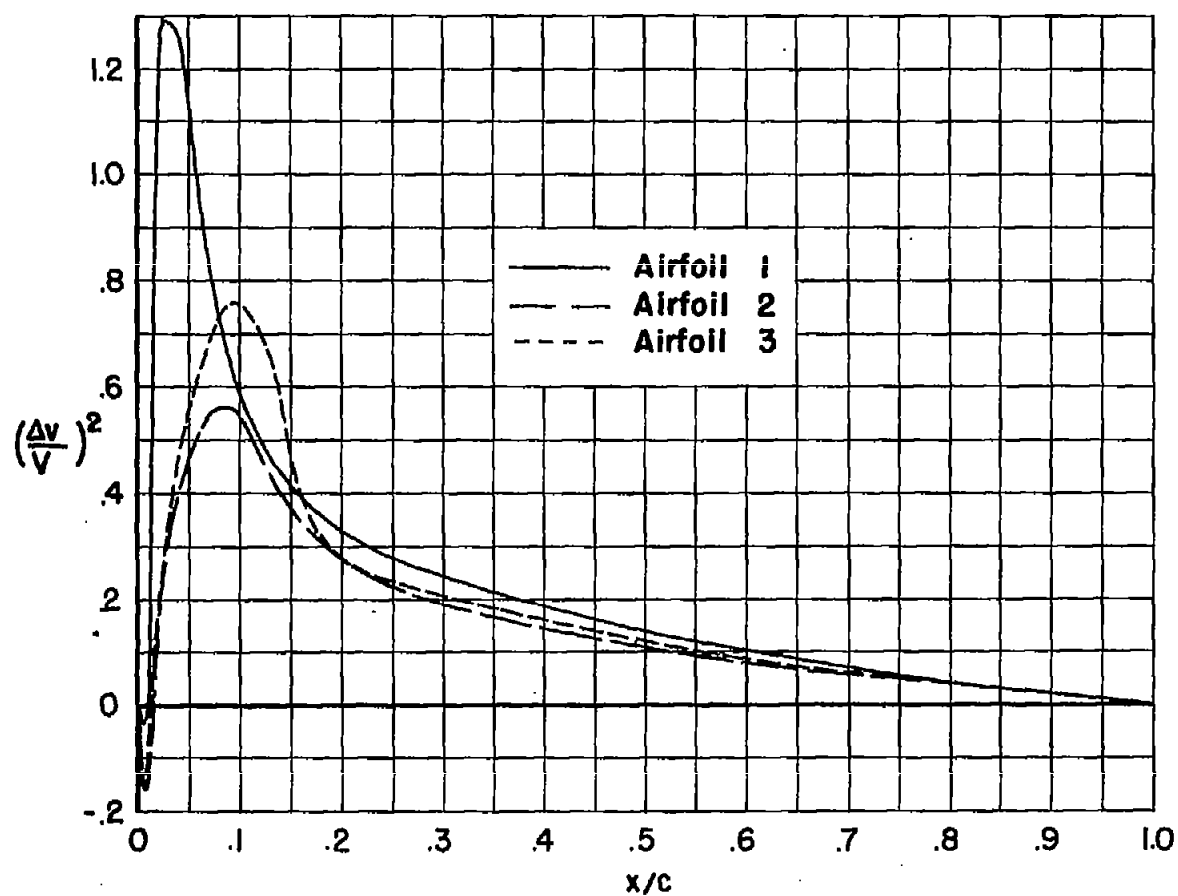


Figure 1.- Profiles of the modified airfoils.



(a) Pressure distributions corresponding to the basic thickness form.

Figure 2.- Pressure-distribution data for the NACA 64A010 section and the modified airfoil sections as computed by the theories of references 8 and 9.



(b) Loading due to camber.

Figure 2.- Concluded.

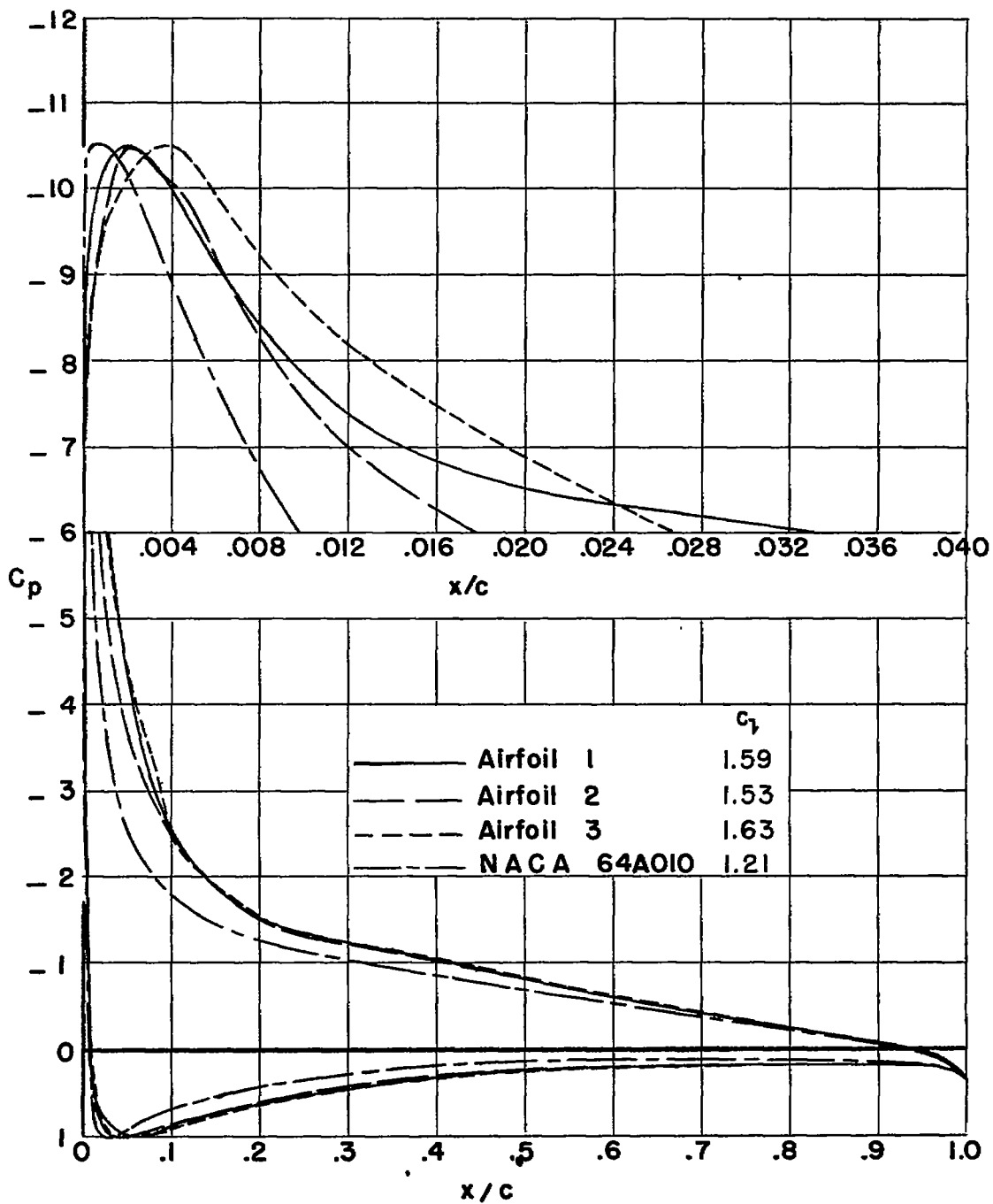
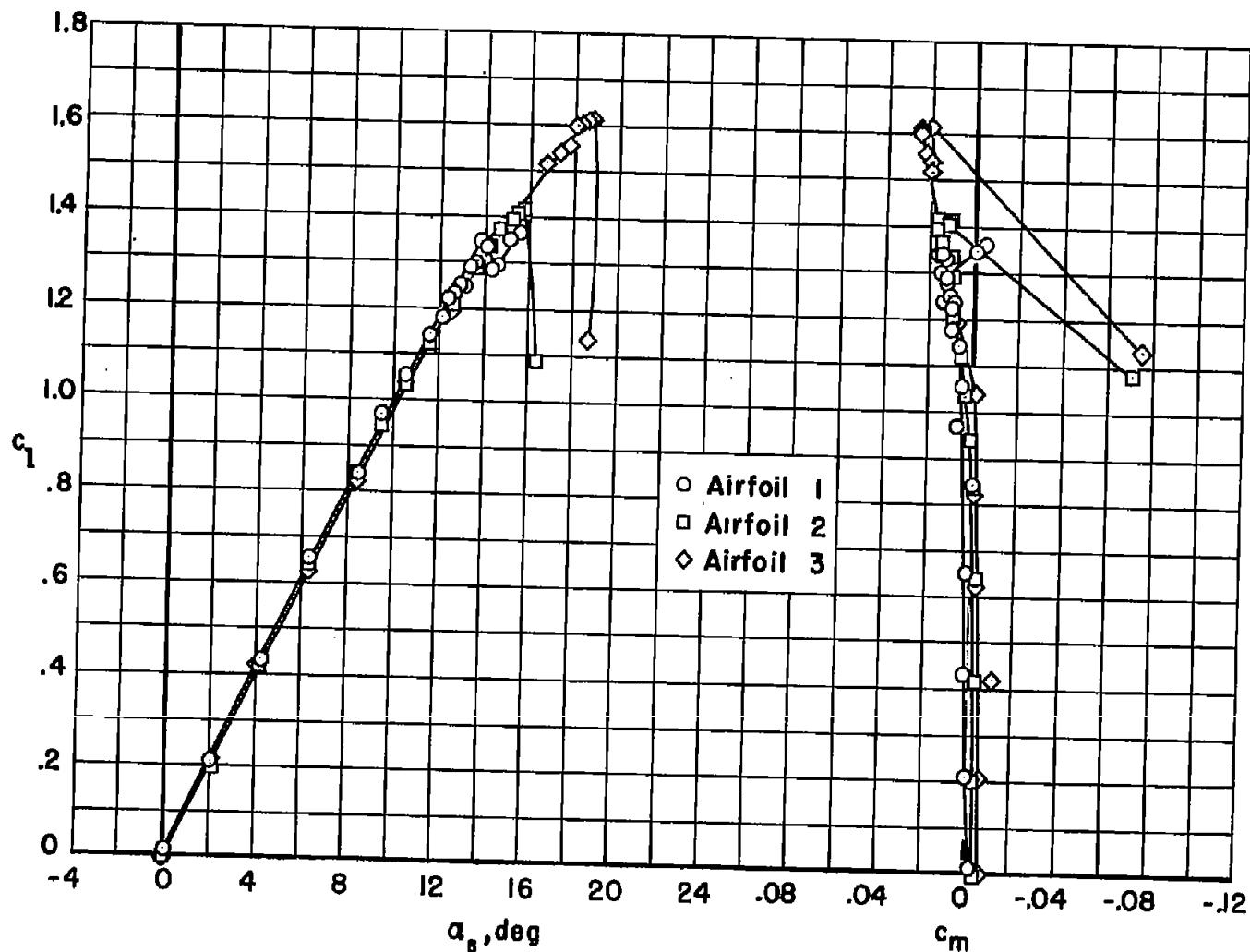
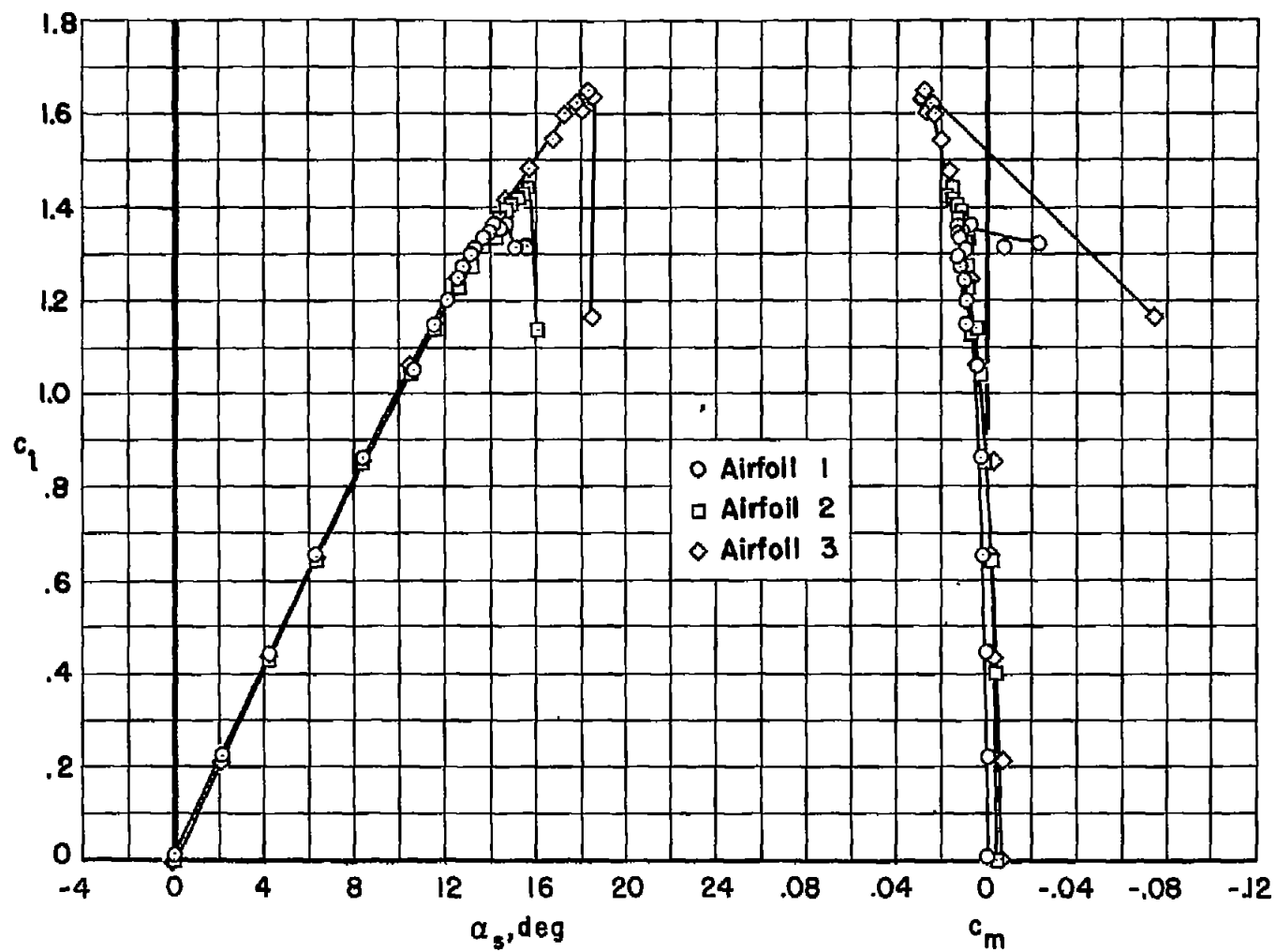


Figure 3.- Pressure distributions at high lift for the NACA 64A010 section and the modified airfoil sections as computed by the theories of references 8 and 9.



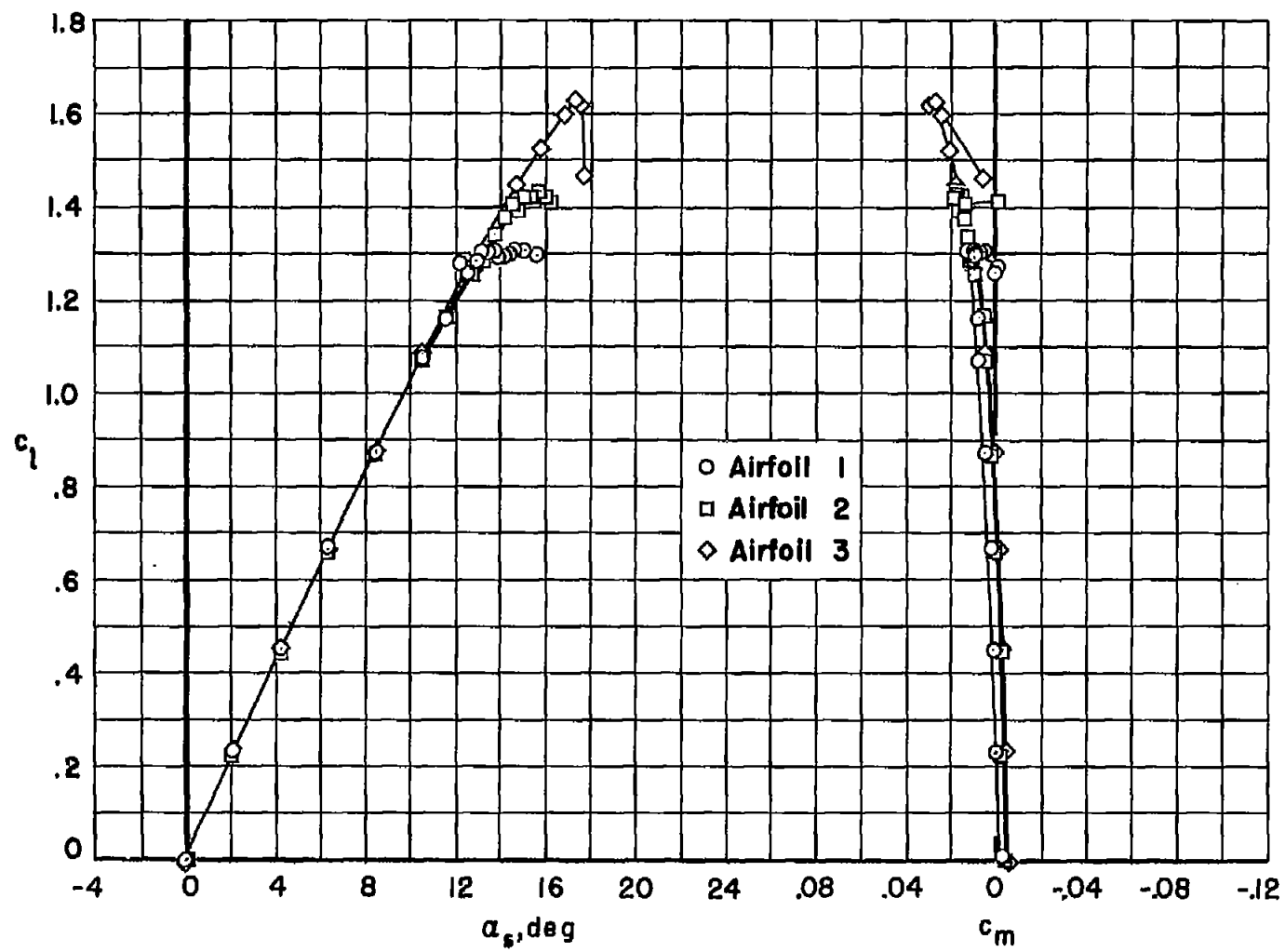
(a) $R = 2.8 \times 10^6$; $M = 0.08$

Figure 4.- Lift and pitching-moment characteristics of the modified airfoil sections at low speeds.



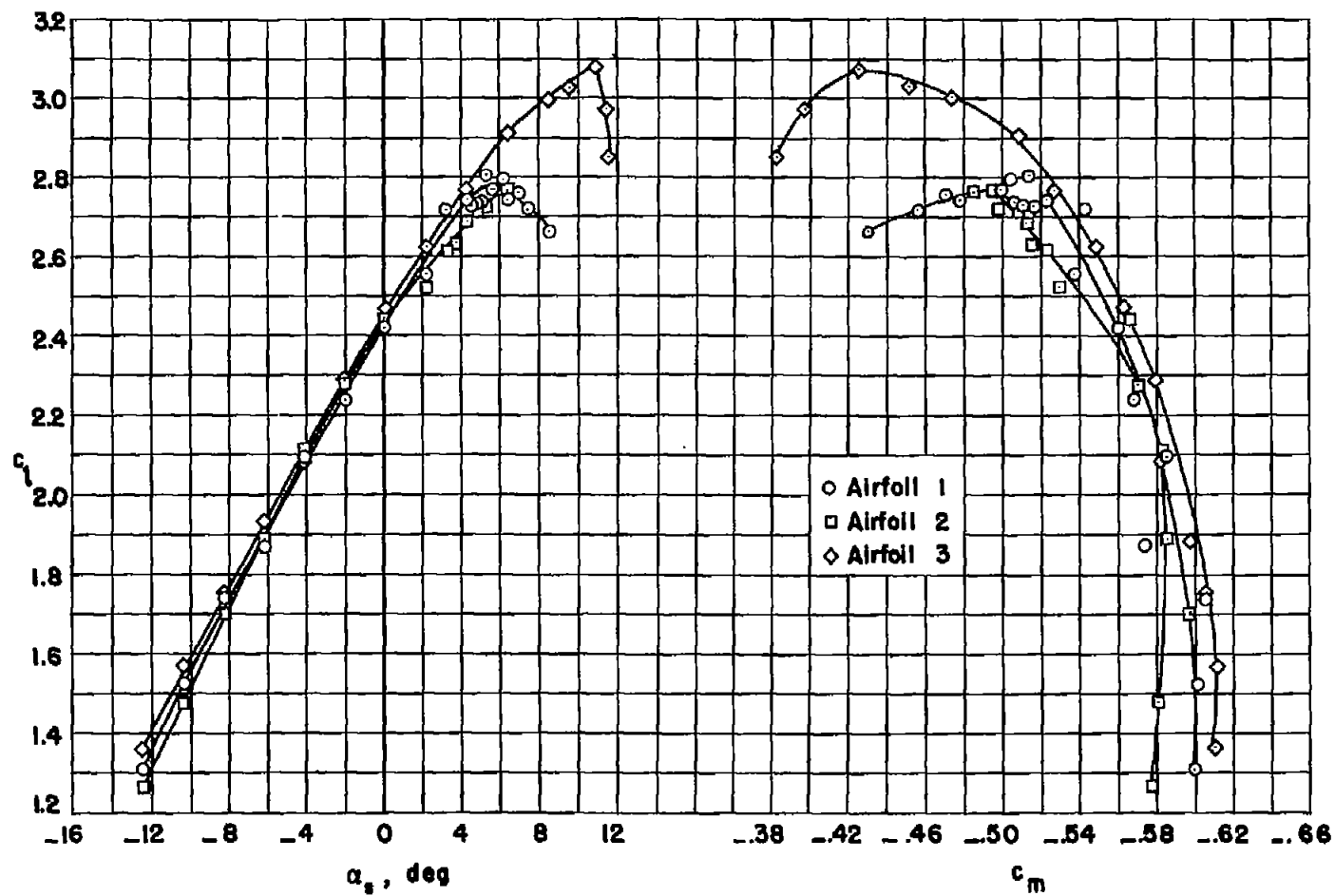
(b) $R = 4.0 \times 10^6$; $M = 0.12$

Figure 4.- Continued.



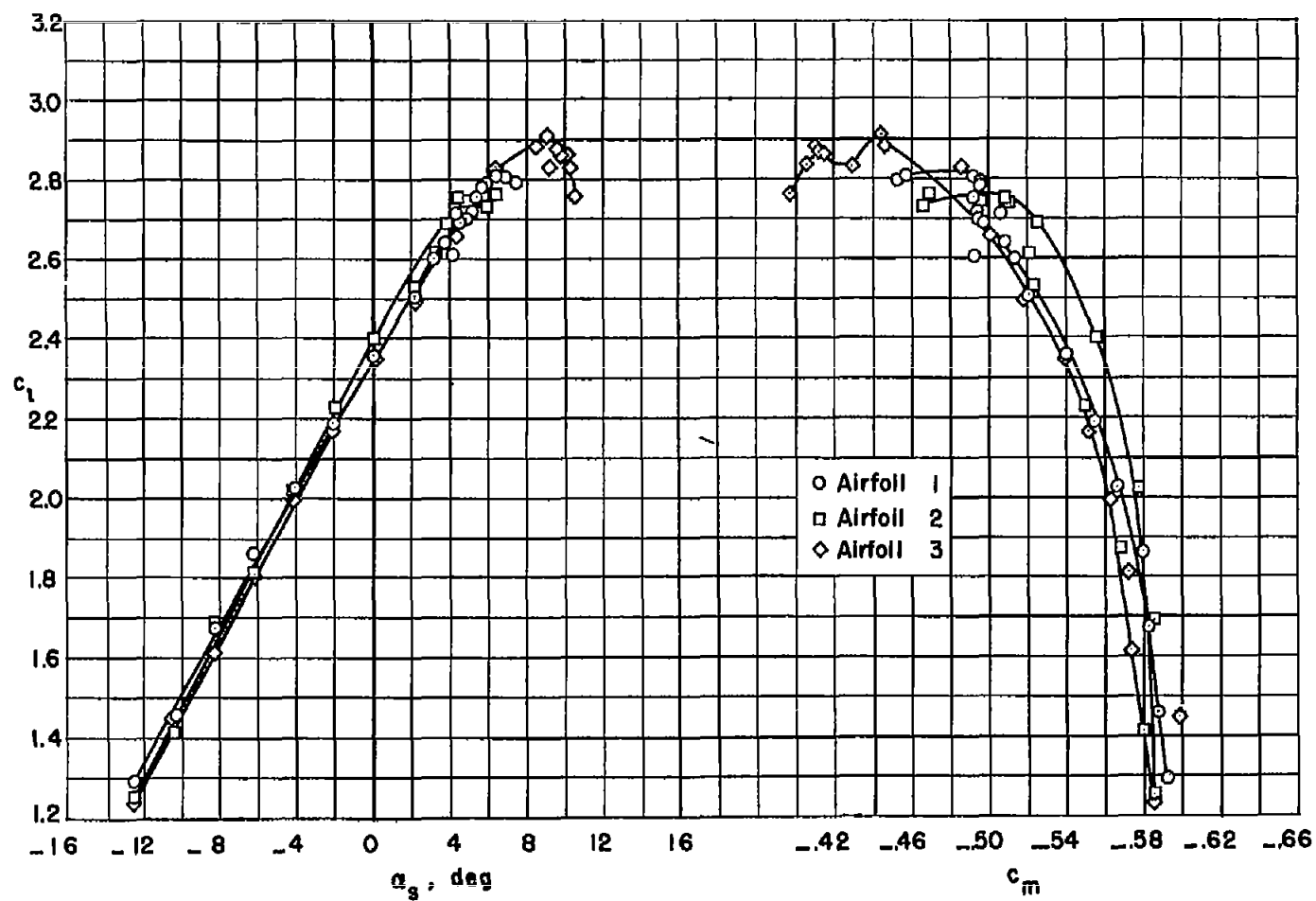
(c) $R = 5.8 \times 10^6$; $M = 0.17$

Figure 4.- Concluded.



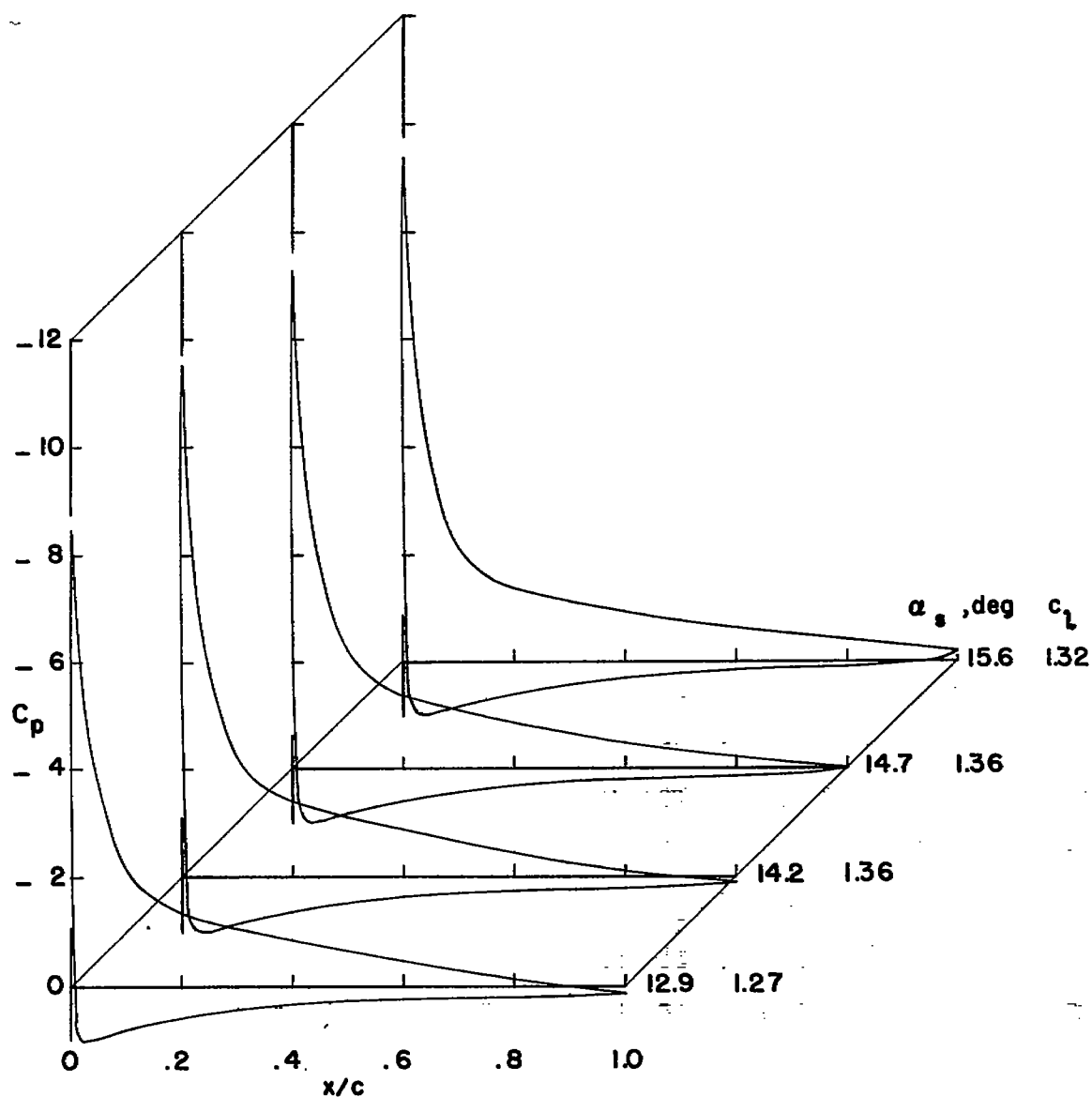
(a) $R = 4.0 \times 10^5$; $M = 0.12$

Figure 5.- Lift and pitching-moment characteristics of the modified airfoil sections at low speeds with double-slotted flaps deflected ($0.25c$ main flap deflected 55°).



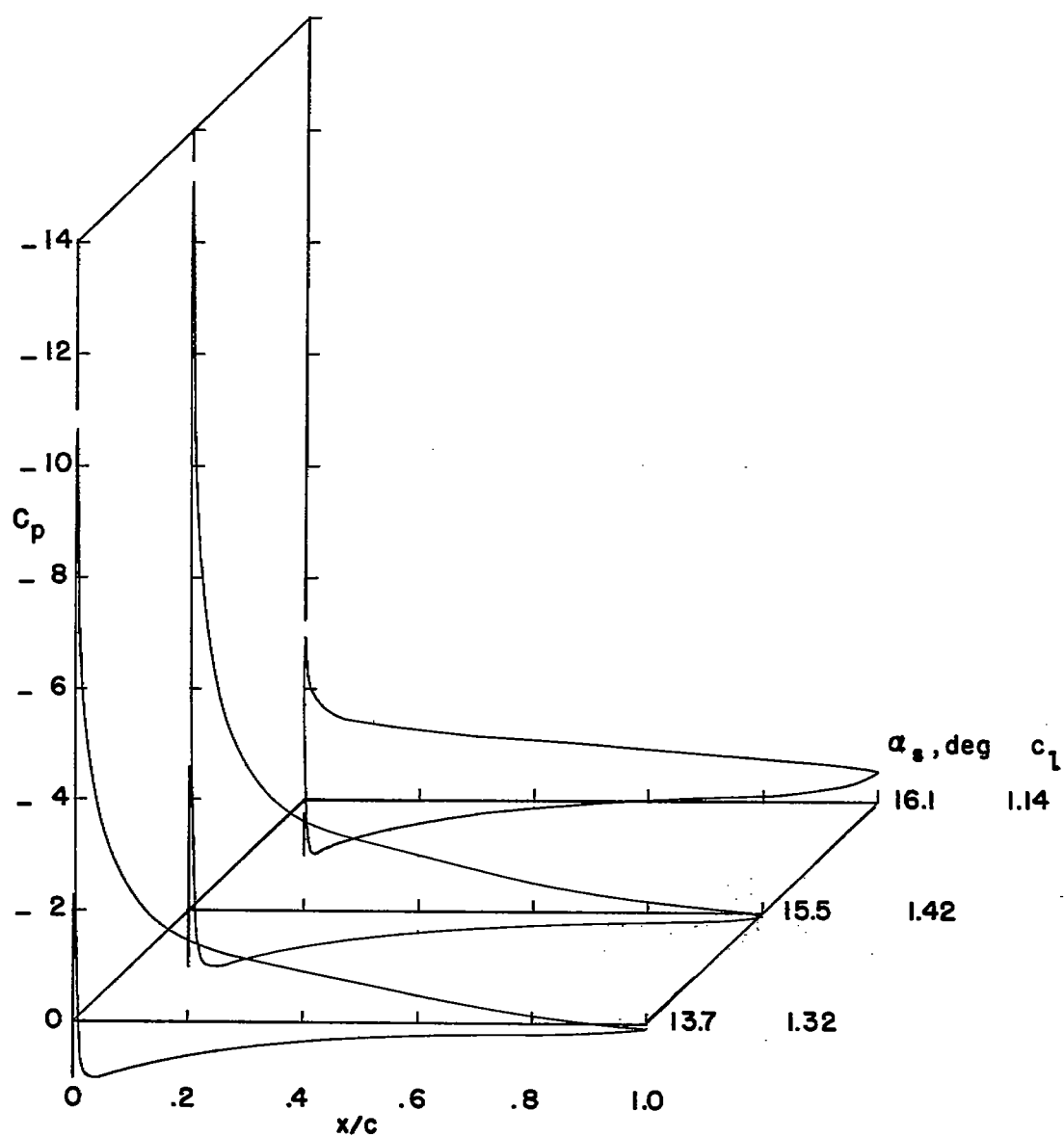
(b) $R = 5.8 \times 10^6$; $M = 0.17$

Figure 5.- Concluded.



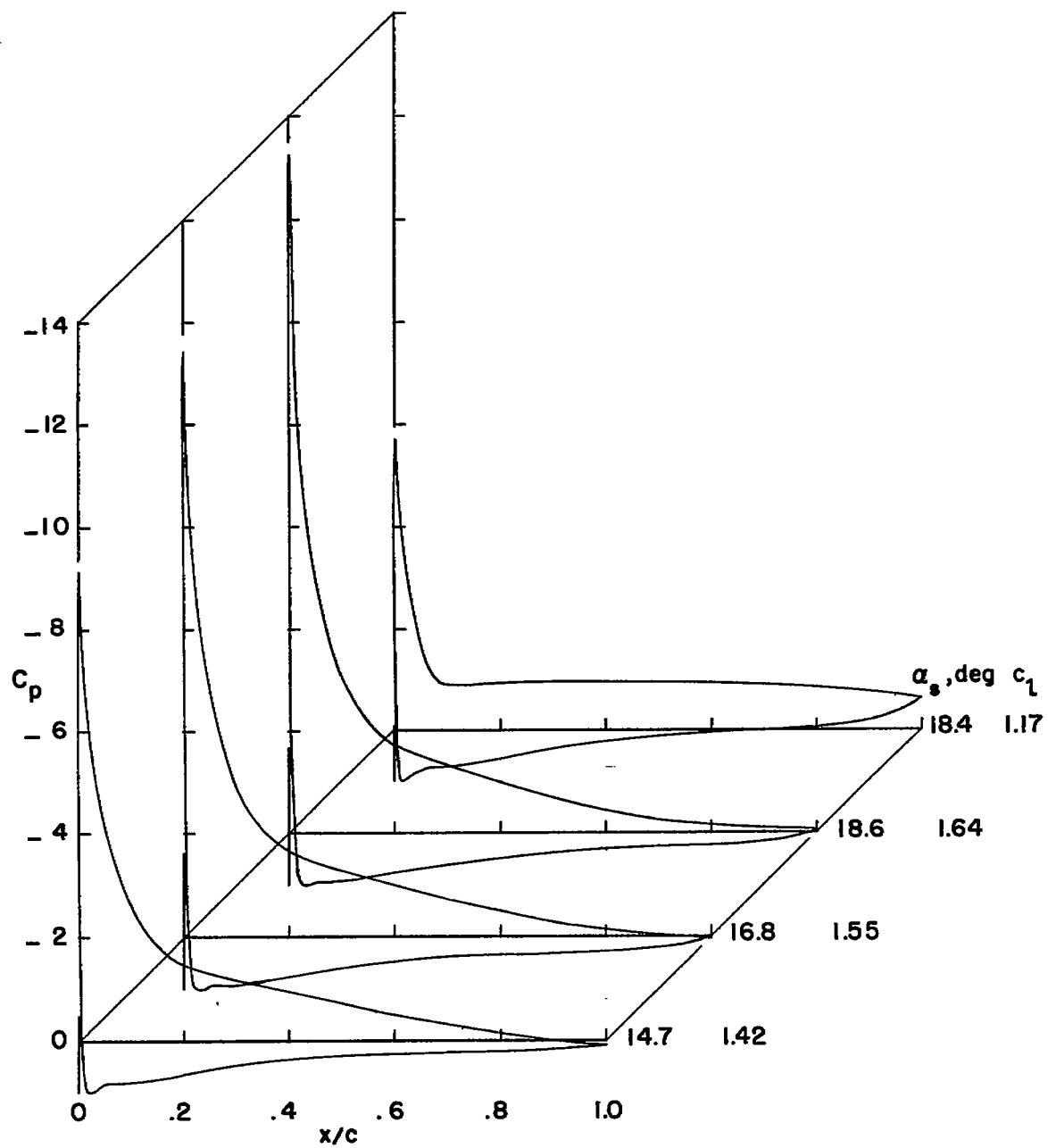
(a) Airfoil 1.

Figure 6.- Experimental pressure distributions near maximum lift;
 $R = 4.0 \times 10^6$, $M = 0.12$.



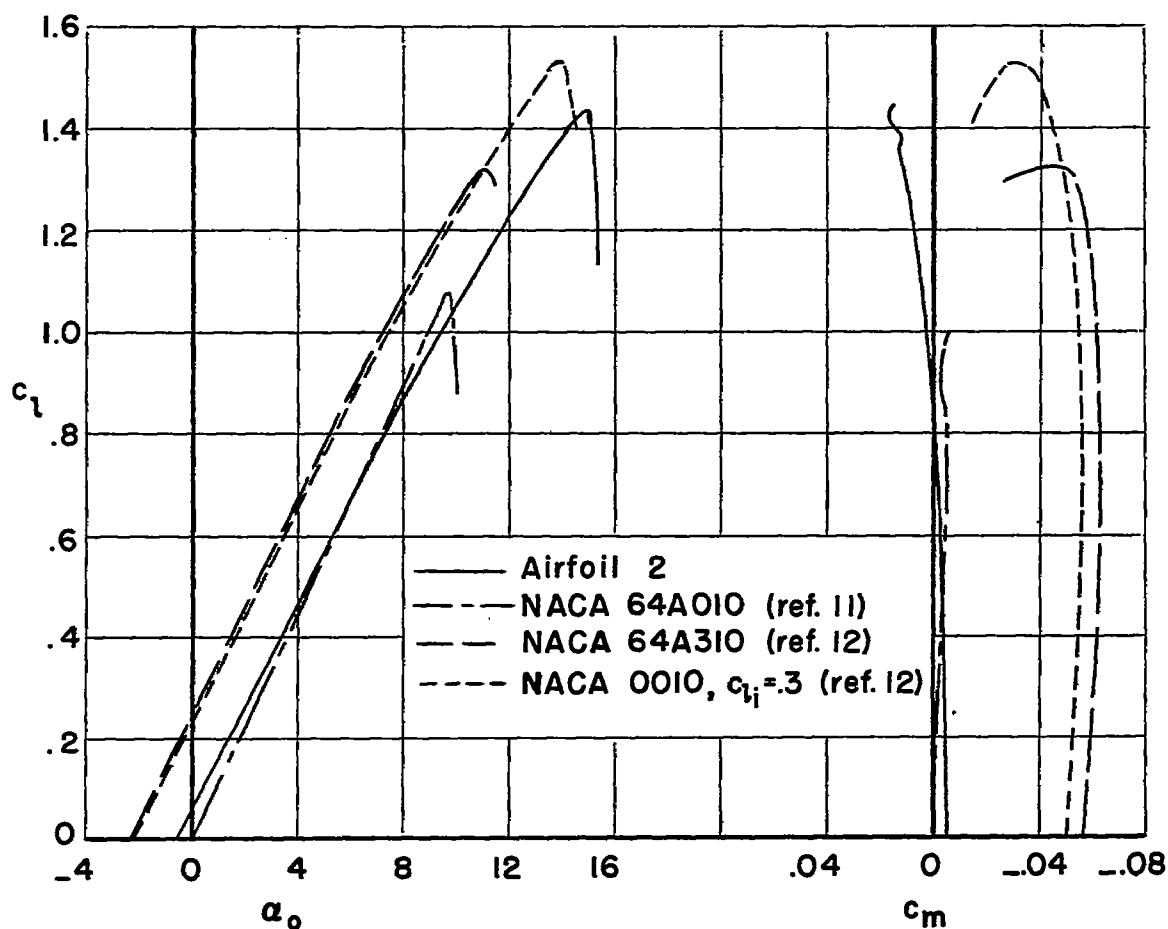
(b) Airfoil 2.

Figure 6.- Continued.



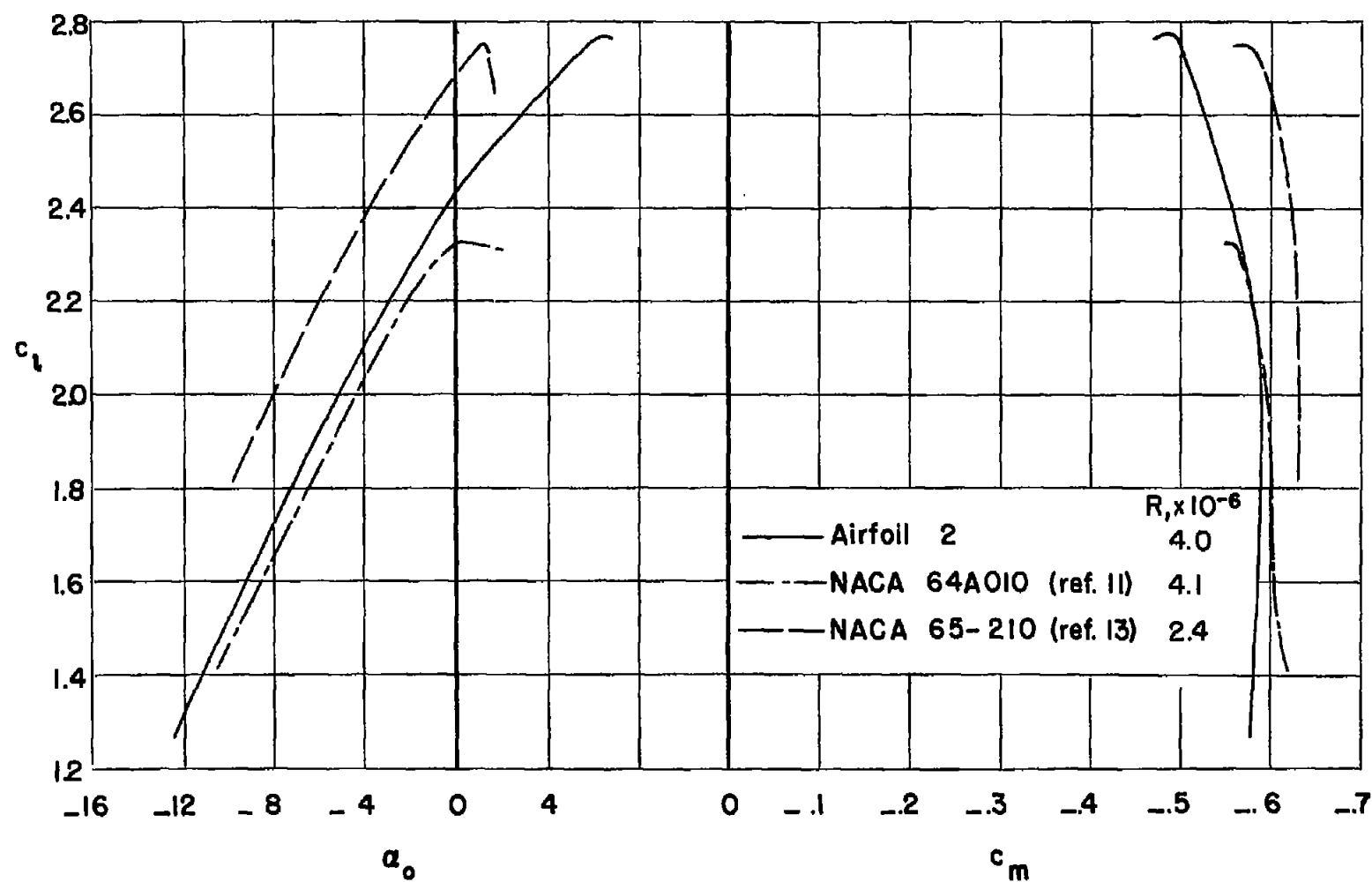
(c) Airfoil 3.

Figure 6.- Concluded.



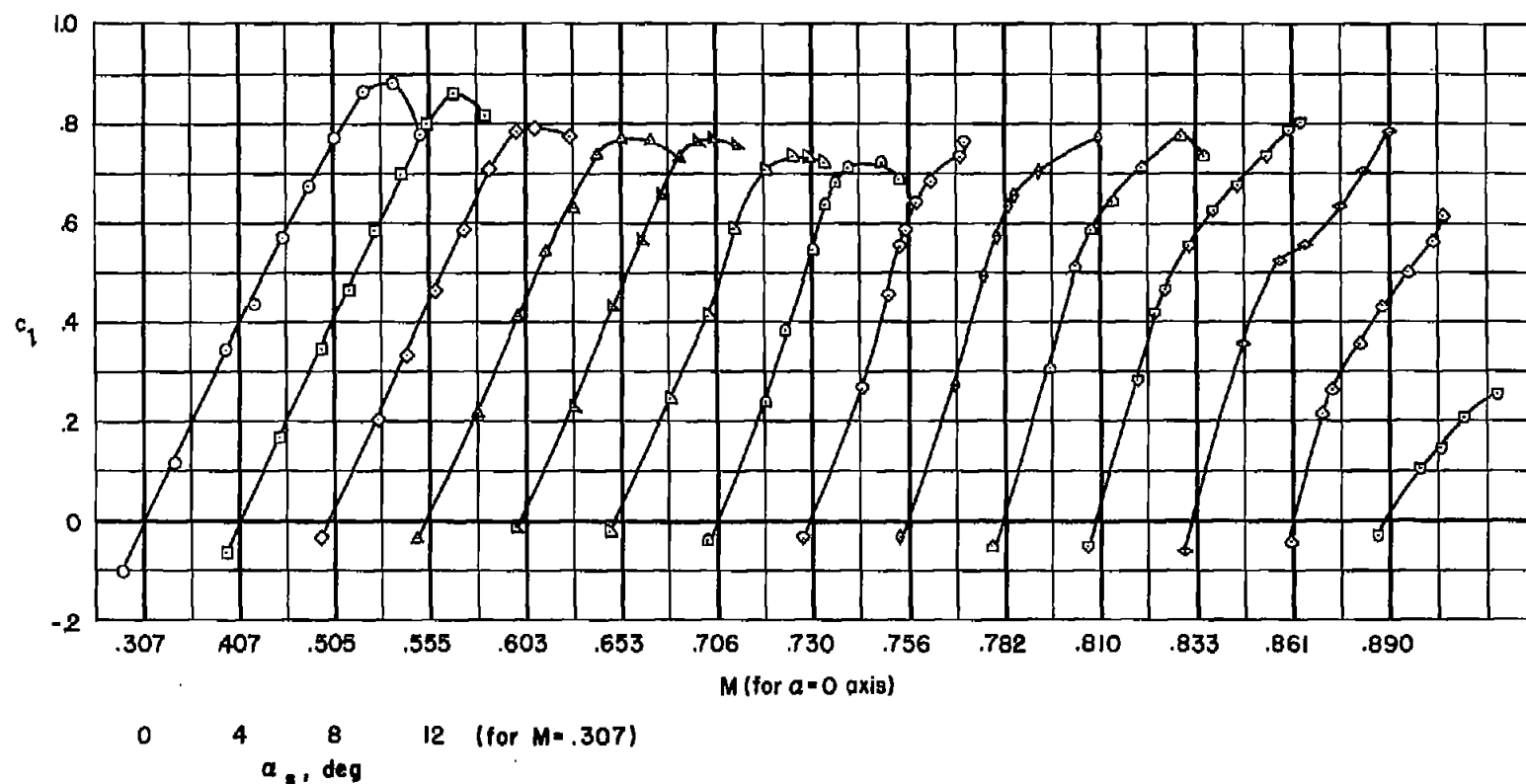
(a) Without flaps; $R = 4 \times 10^6$.

Figure 7.- Comparison of the aerodynamic characteristics of airfoil 2 with a symmetrical section and with a distributed-camber section.



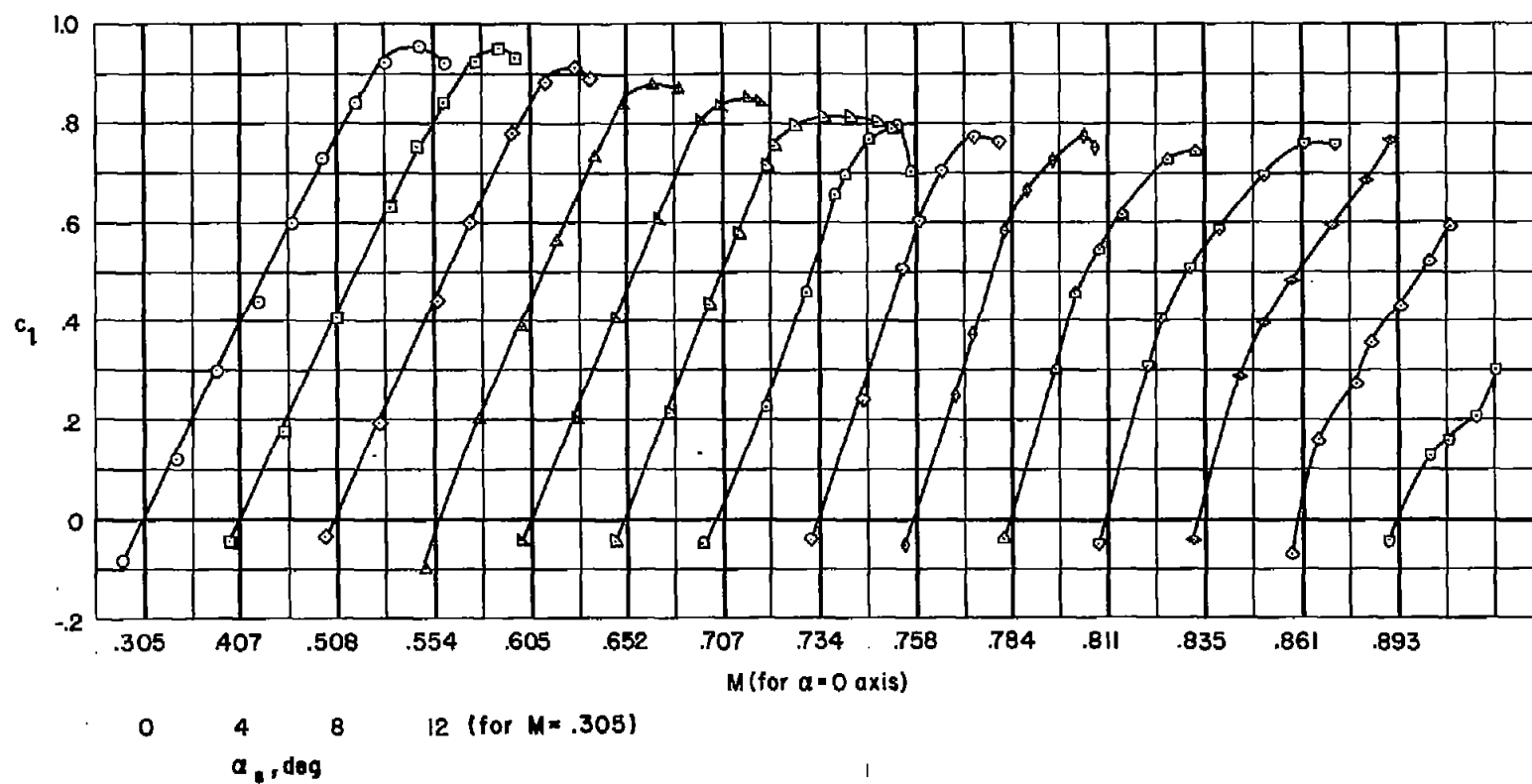
(b) With double-slotted flaps deflected 55° .

Figure 7.- Concluded.



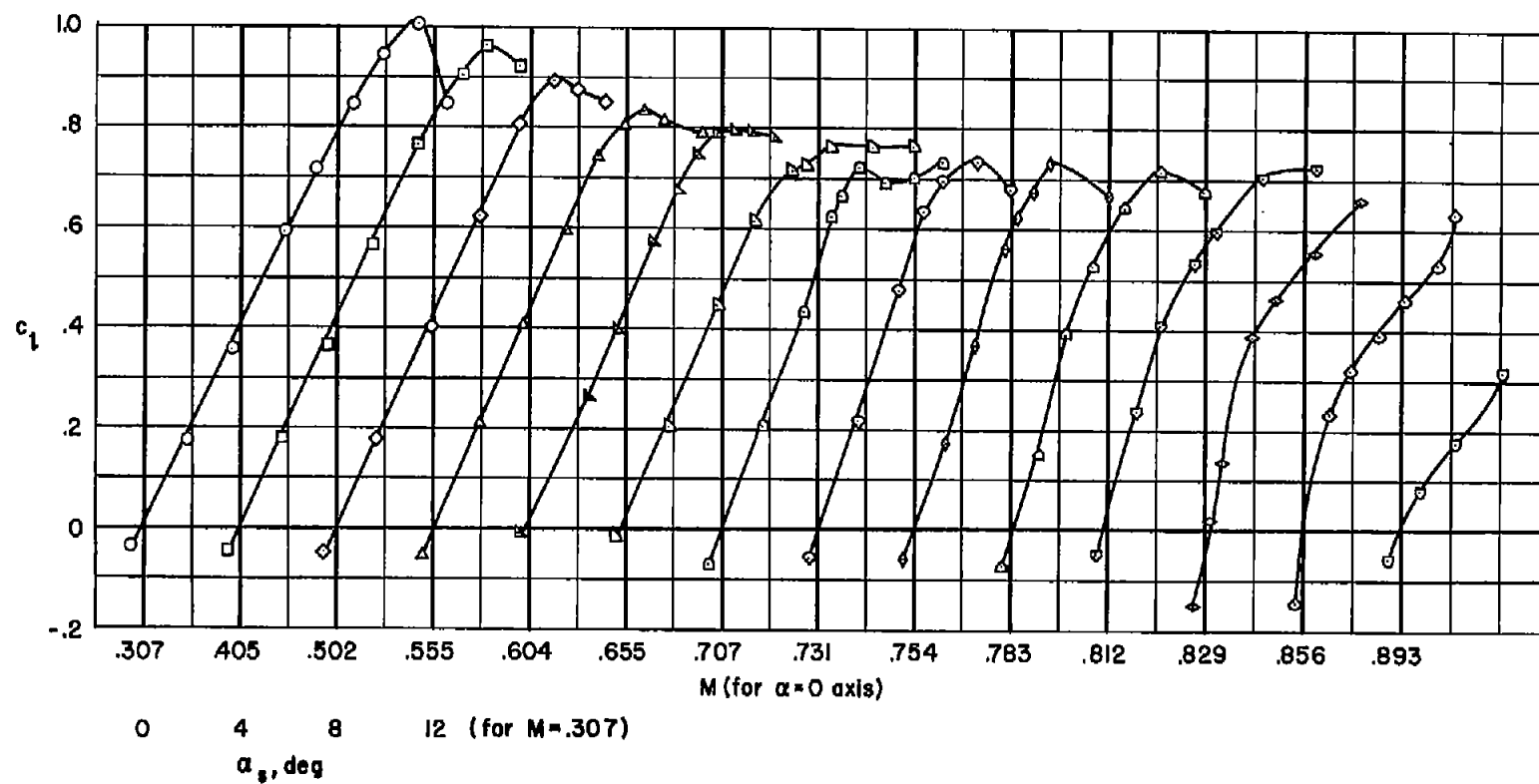
(a) Airfoil 1.

Figure 8.- Lift characteristics of the modified airfoils at various Mach numbers.



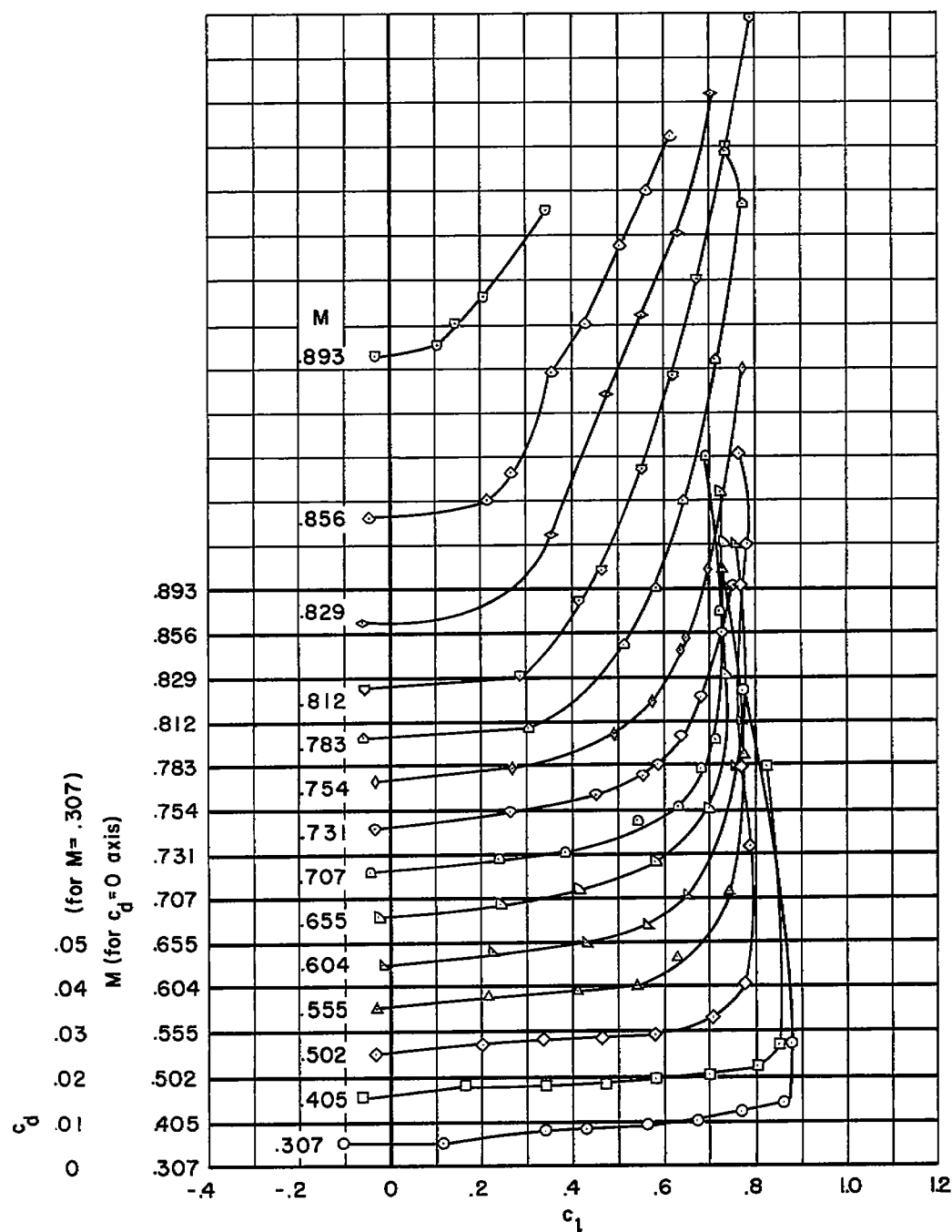
(b) Airfoil 2.

Figure 8.- Continued.



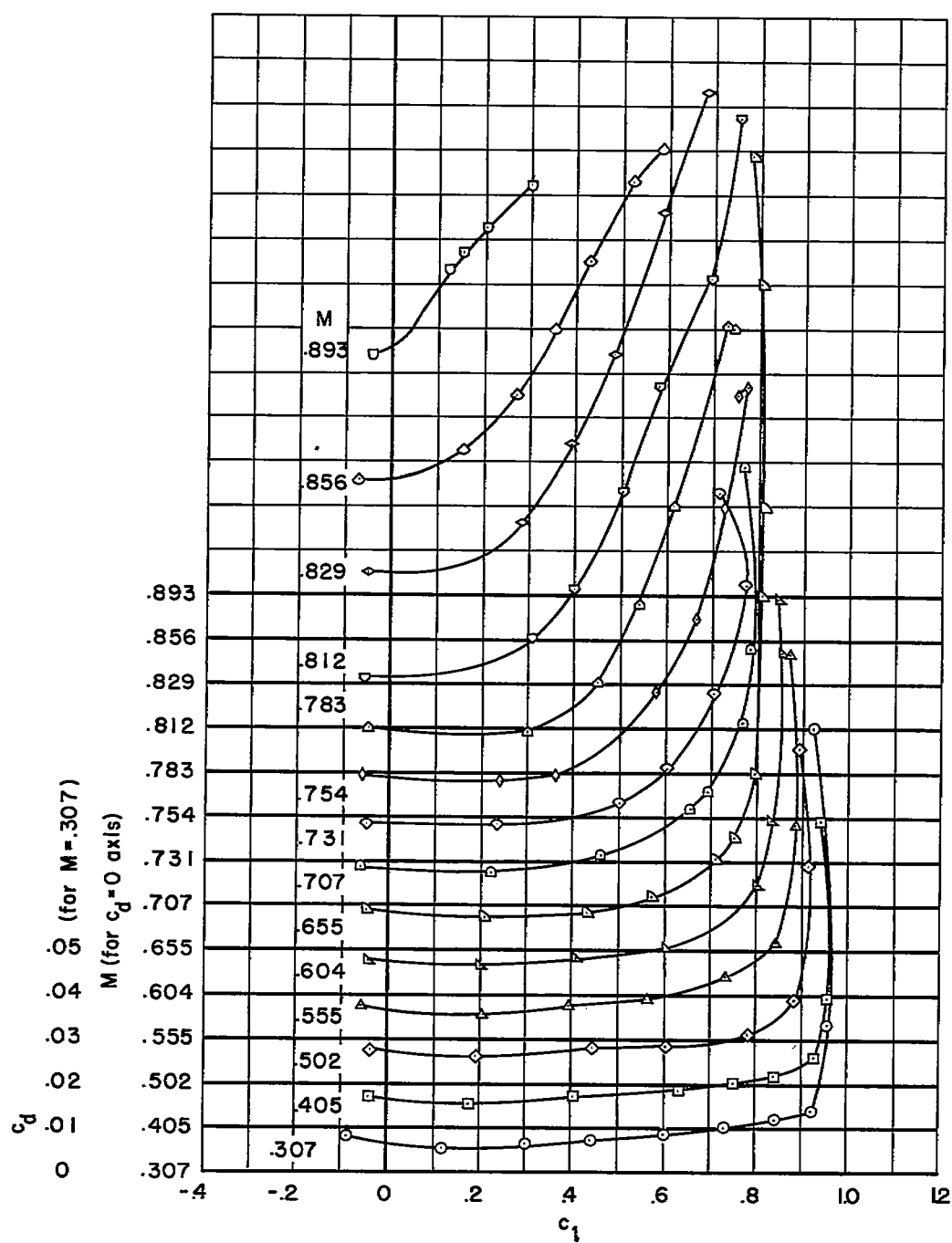
(c) Airfoil 3.

Figure 8.- Concluded.



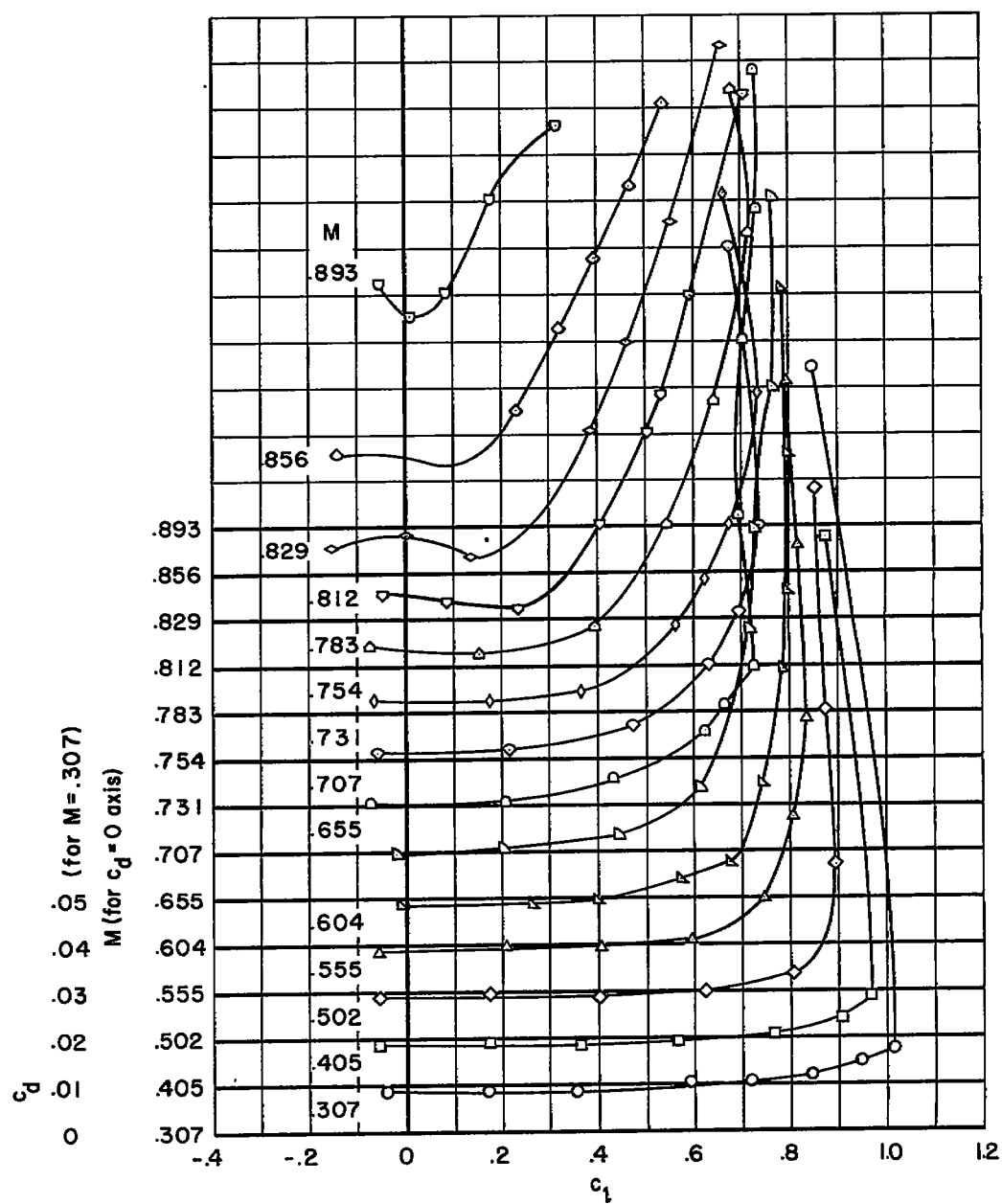
(a) Airfoil 1.

Figure 9.- Drag characteristics of the modified airfoils at various Mach numbers.



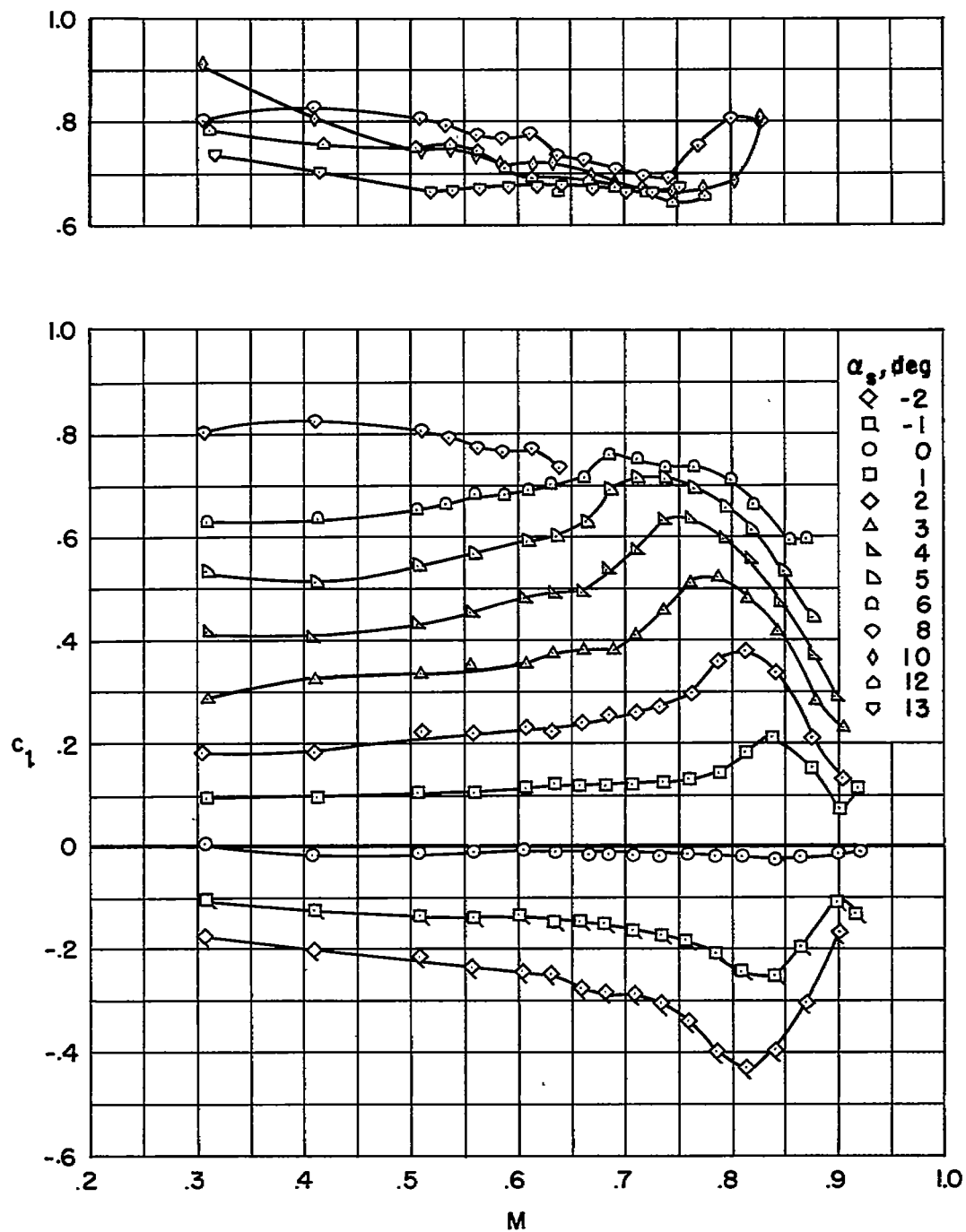
(b) Airfoil 2.

Figure 9.- Continued.



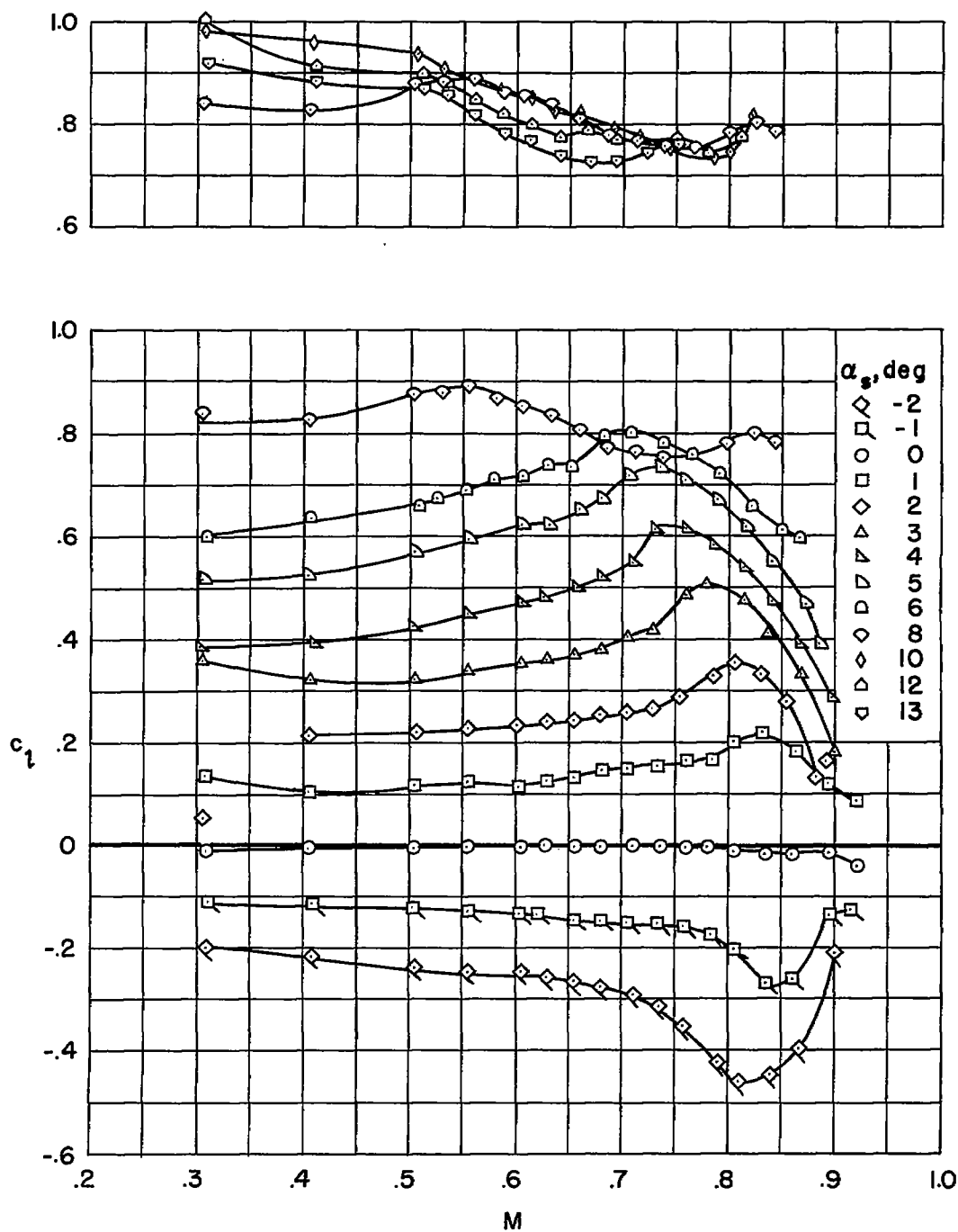
(c) Airfoil 3.

Figure 9.- Concluded.



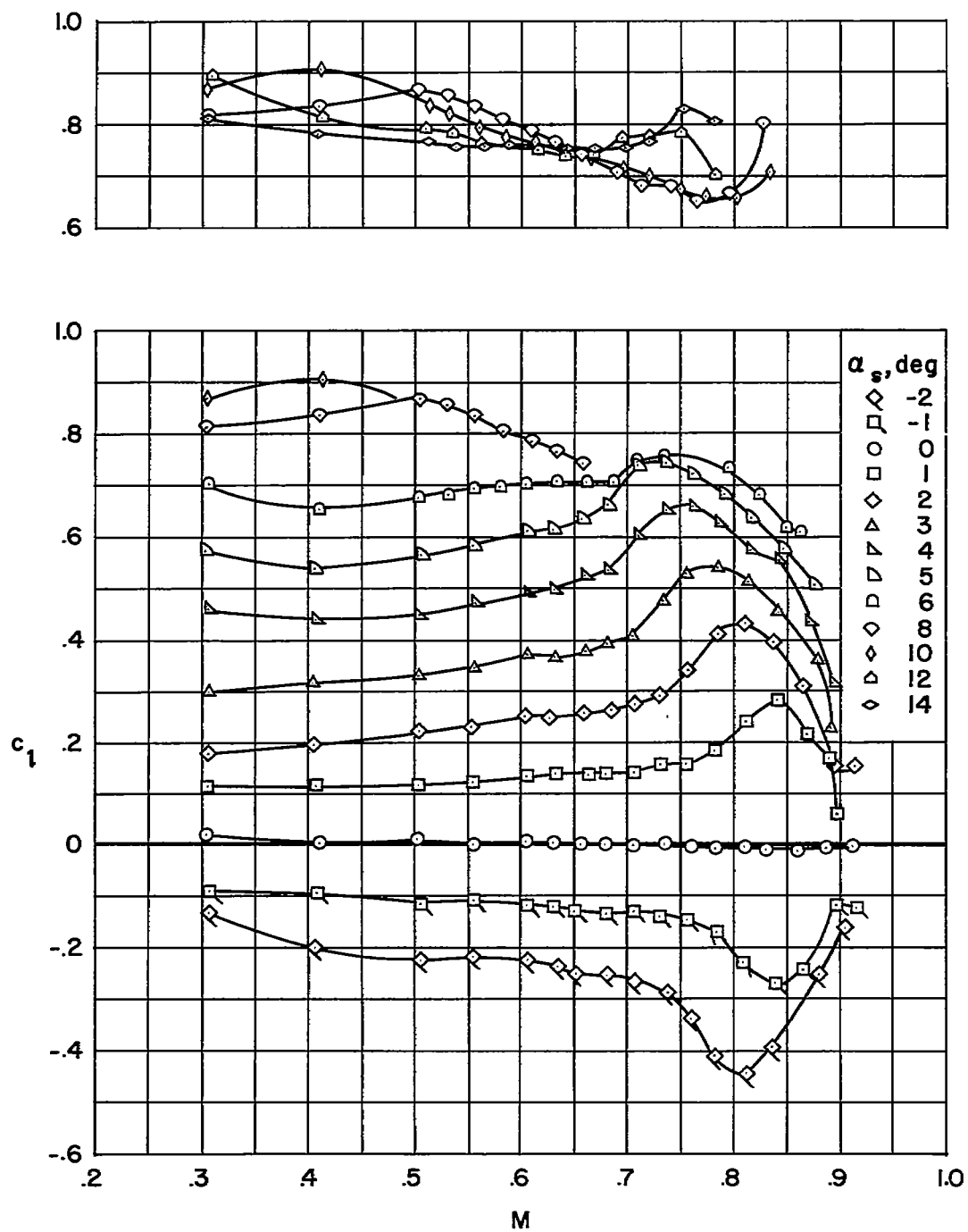
(a) Airfoil 1.

Figure 10.- Lift characteristics of the modified airfoils at various angles of attack.



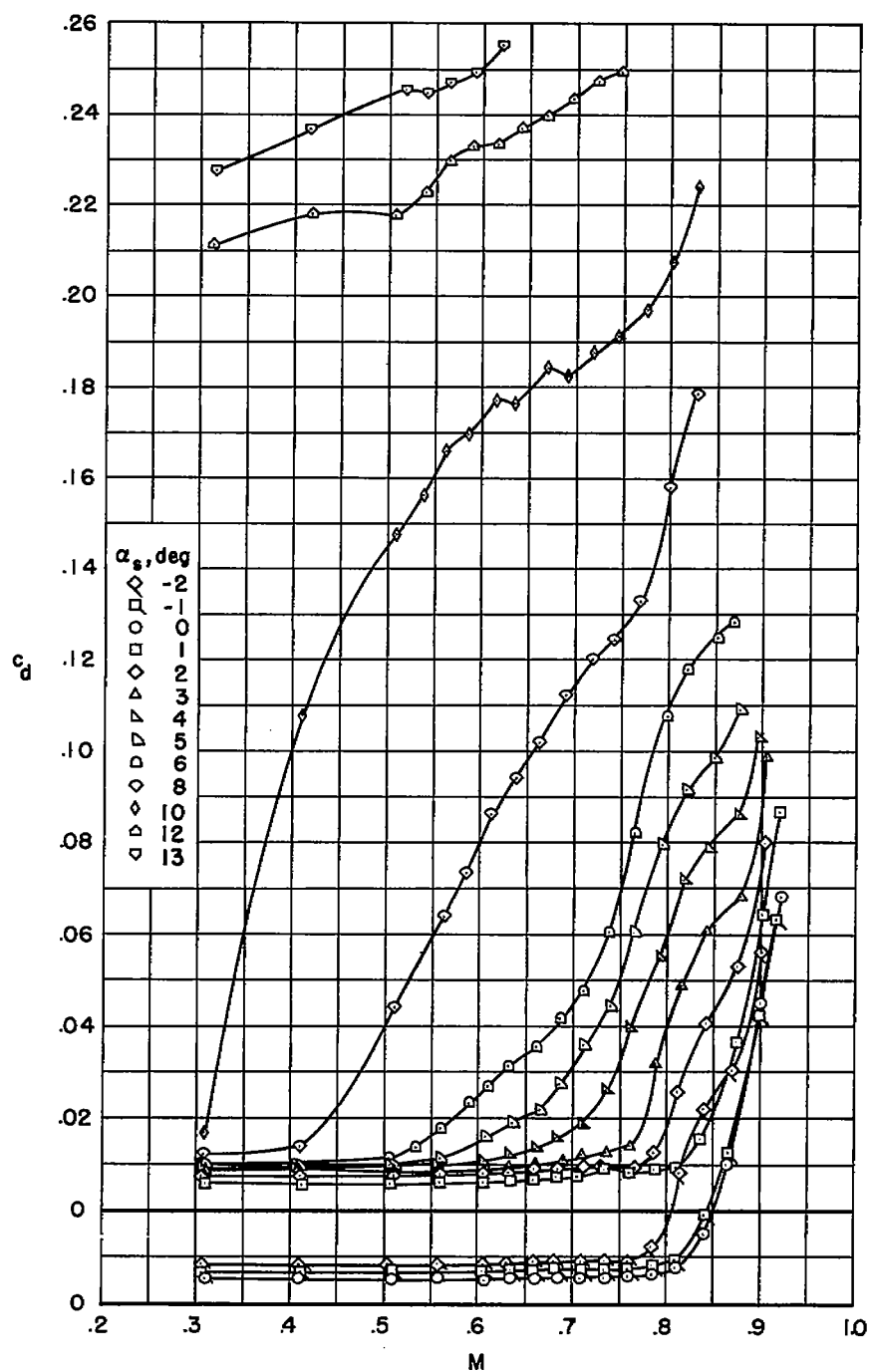
(b) Airfoil 2.

Figure 10.- Continued.



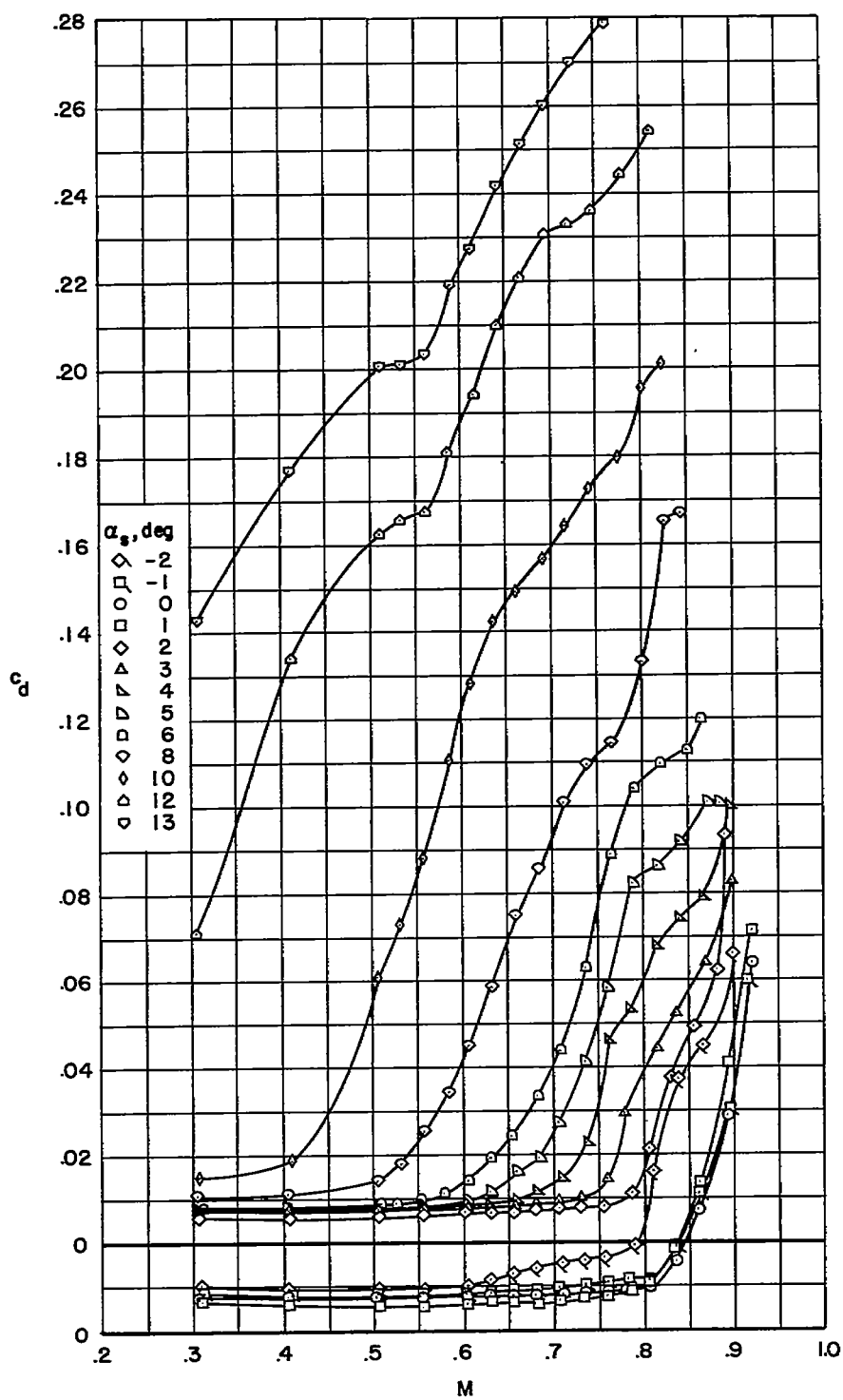
(c) Airfoil 3.

Figure 10.- Concluded.



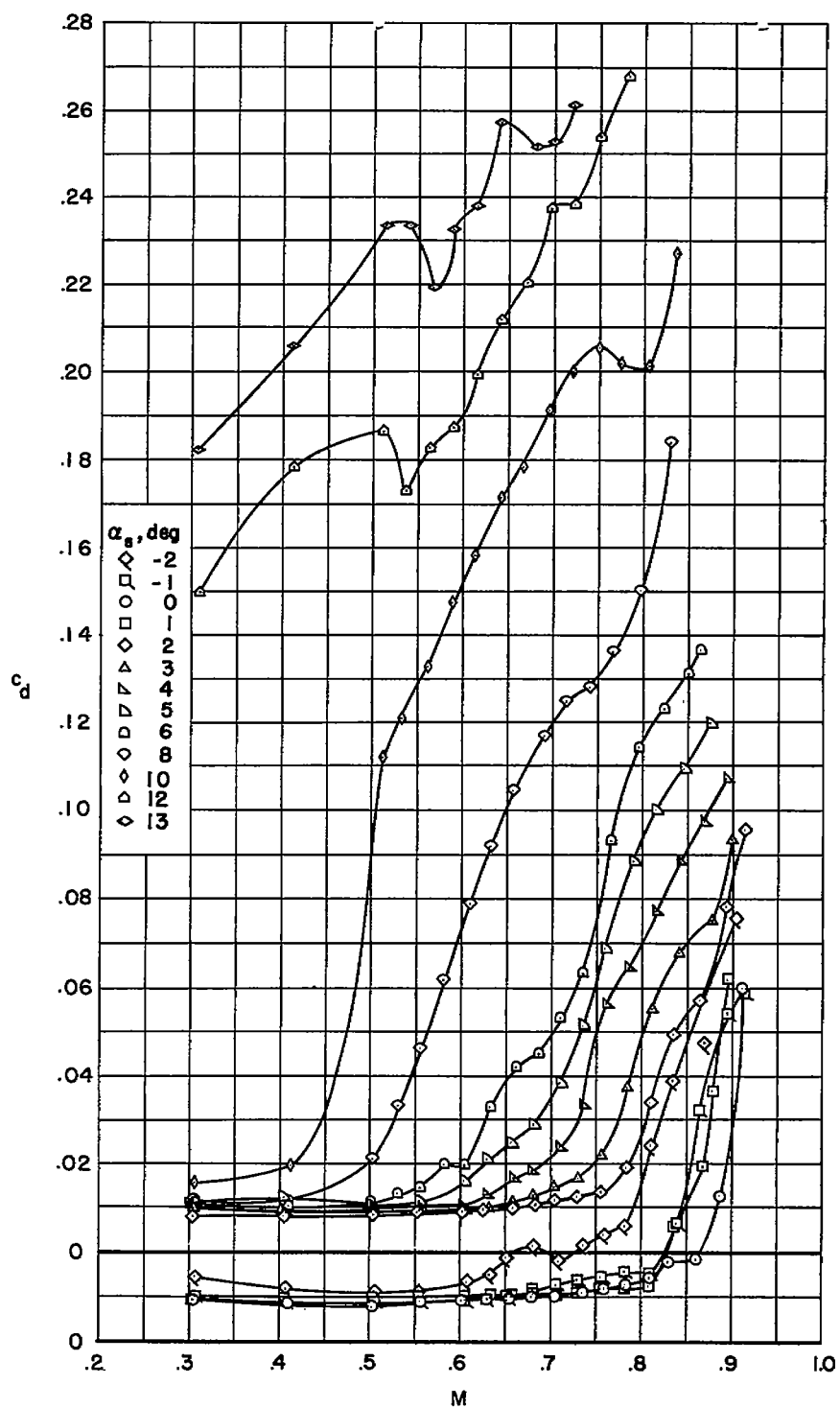
(a) Airfoil 1.

Figure 11.- Drag characteristics of the modified airfoils at various angles of attack.



(b) Airfoil 2.

Figure 11.- Continued.



(c) Airfoil 3.

Figure 11.- Concluded.

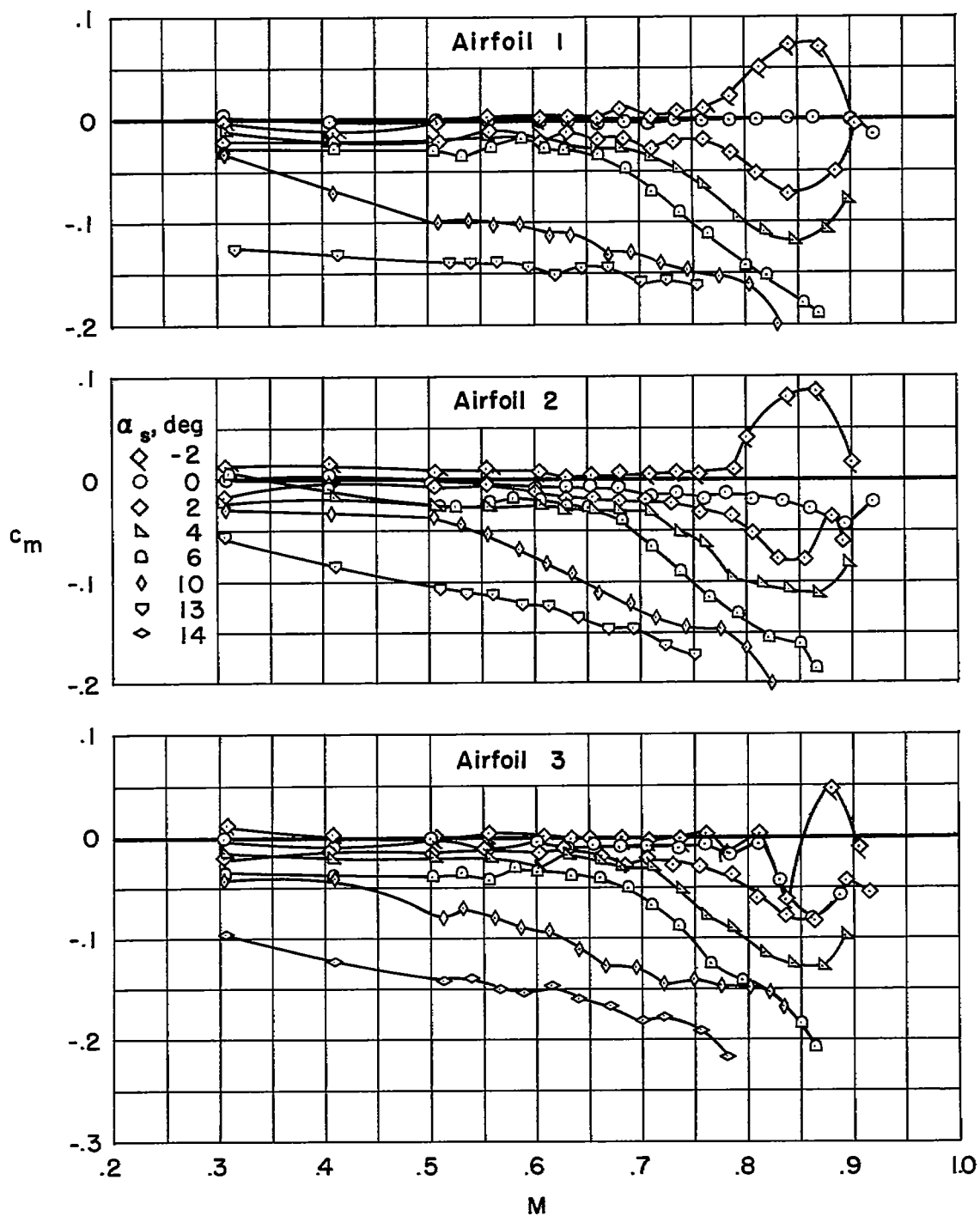


Figure 12.- Pitching-moment characteristics of the modified airfoils at various angles of attack.

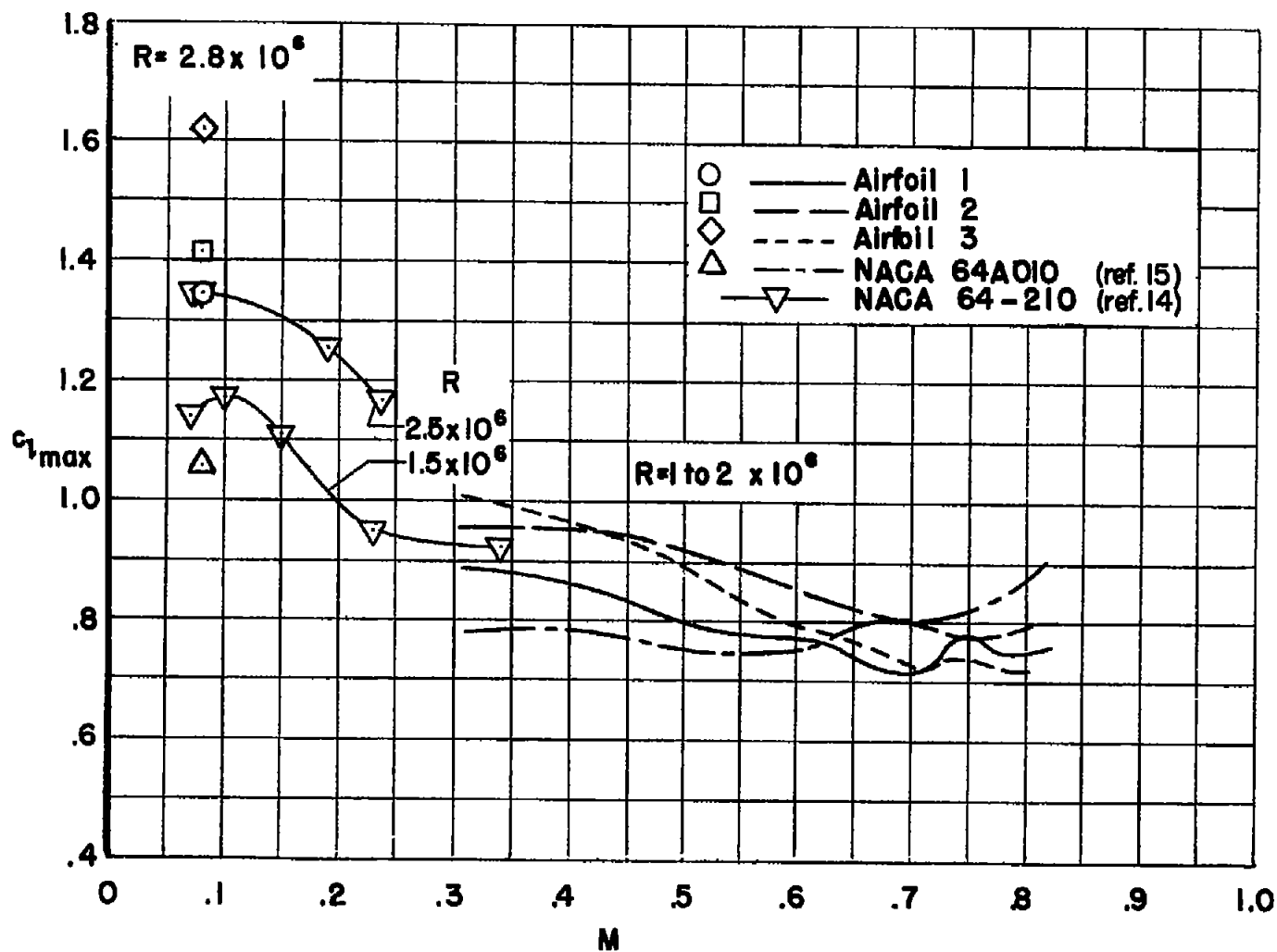
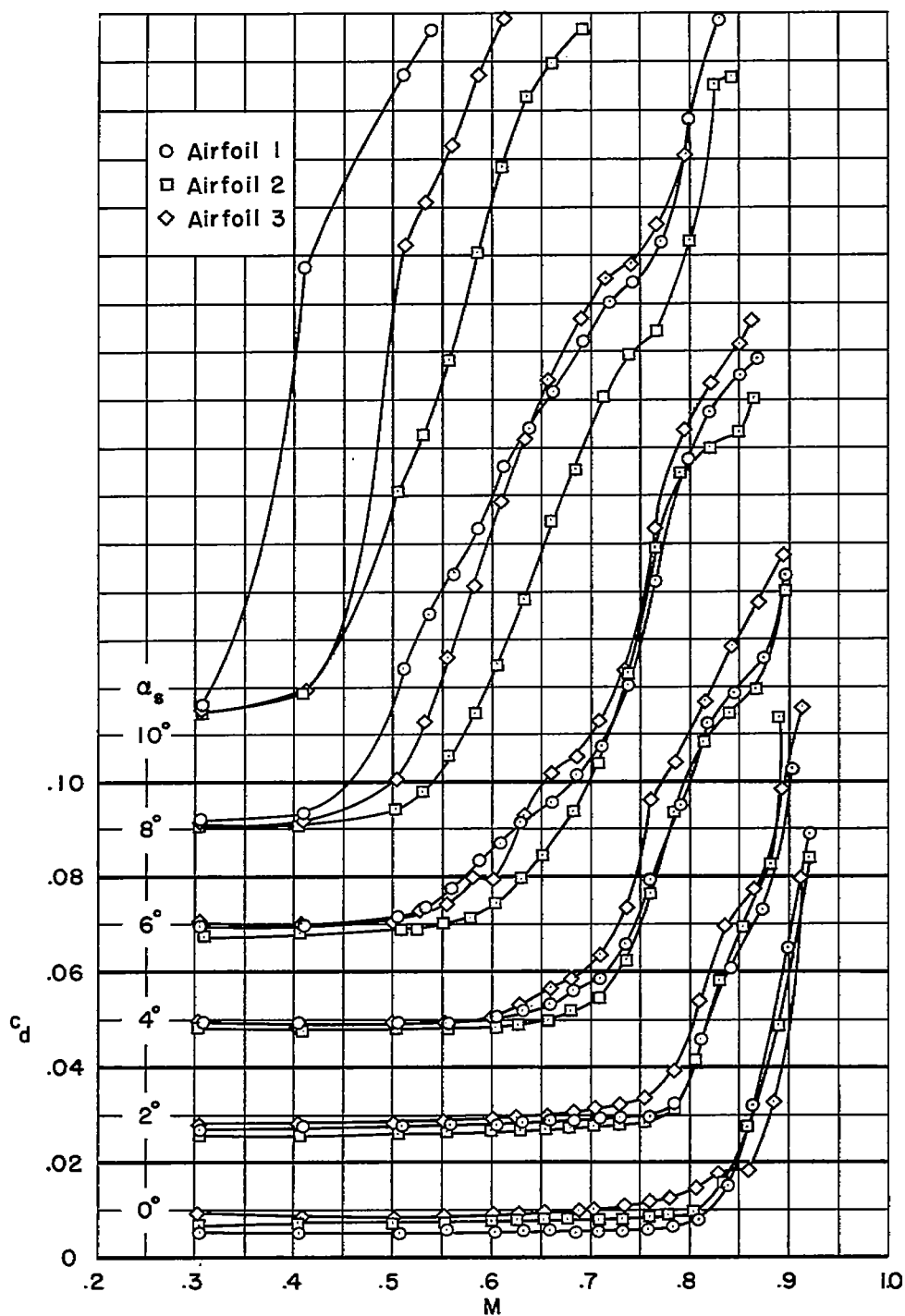
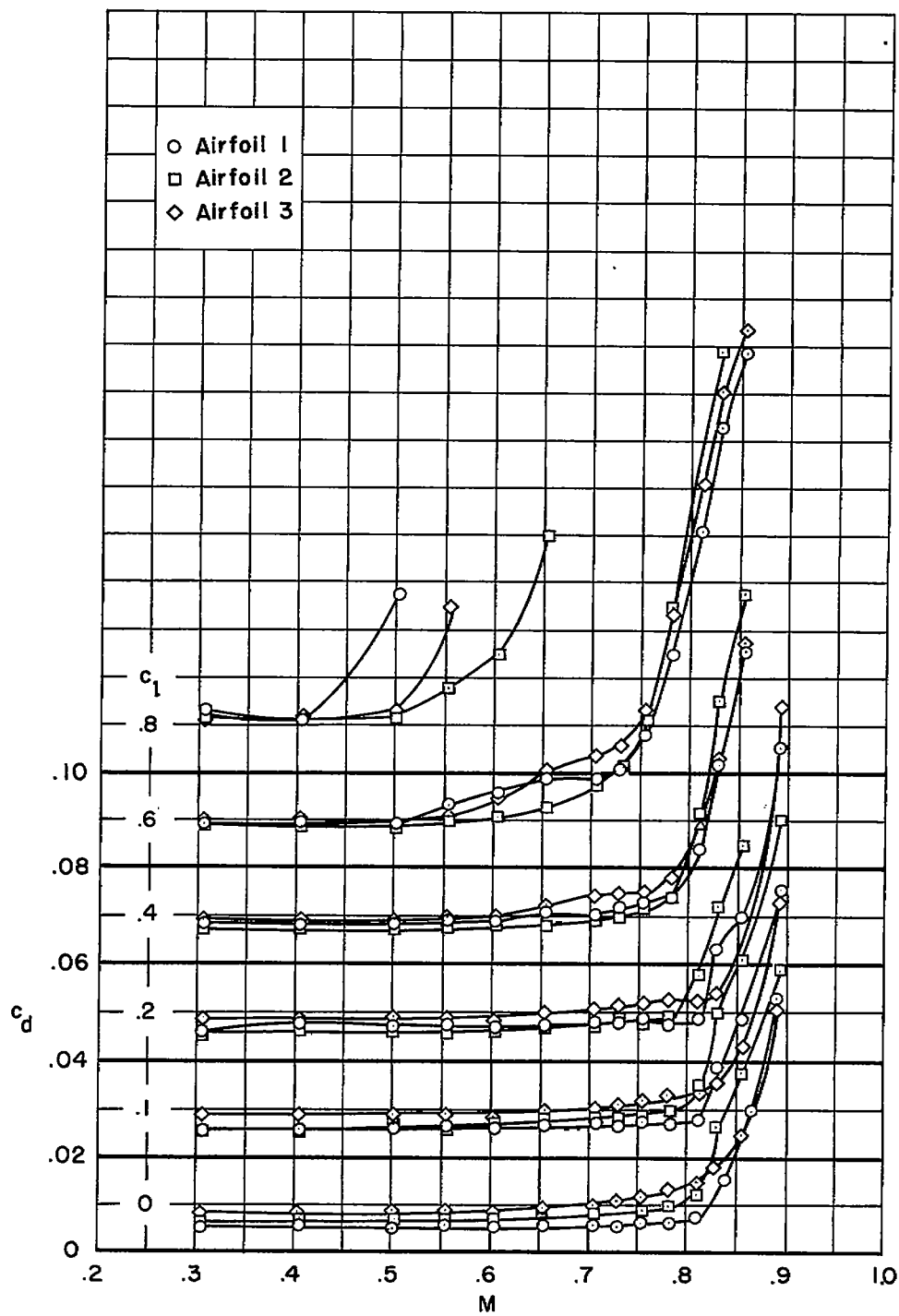


Figure 13.- Variation of $c_{l_{max}}$ with Mach number of the NACA 64A010 and 64-210 sections and the modified airfoil sections.



(a) At selected angles of attack.

Figure 14.- Comparison of the drag characteristics of the modified airfoils.



(b) At selected lift coefficients.

Figure 14.- Concluded.

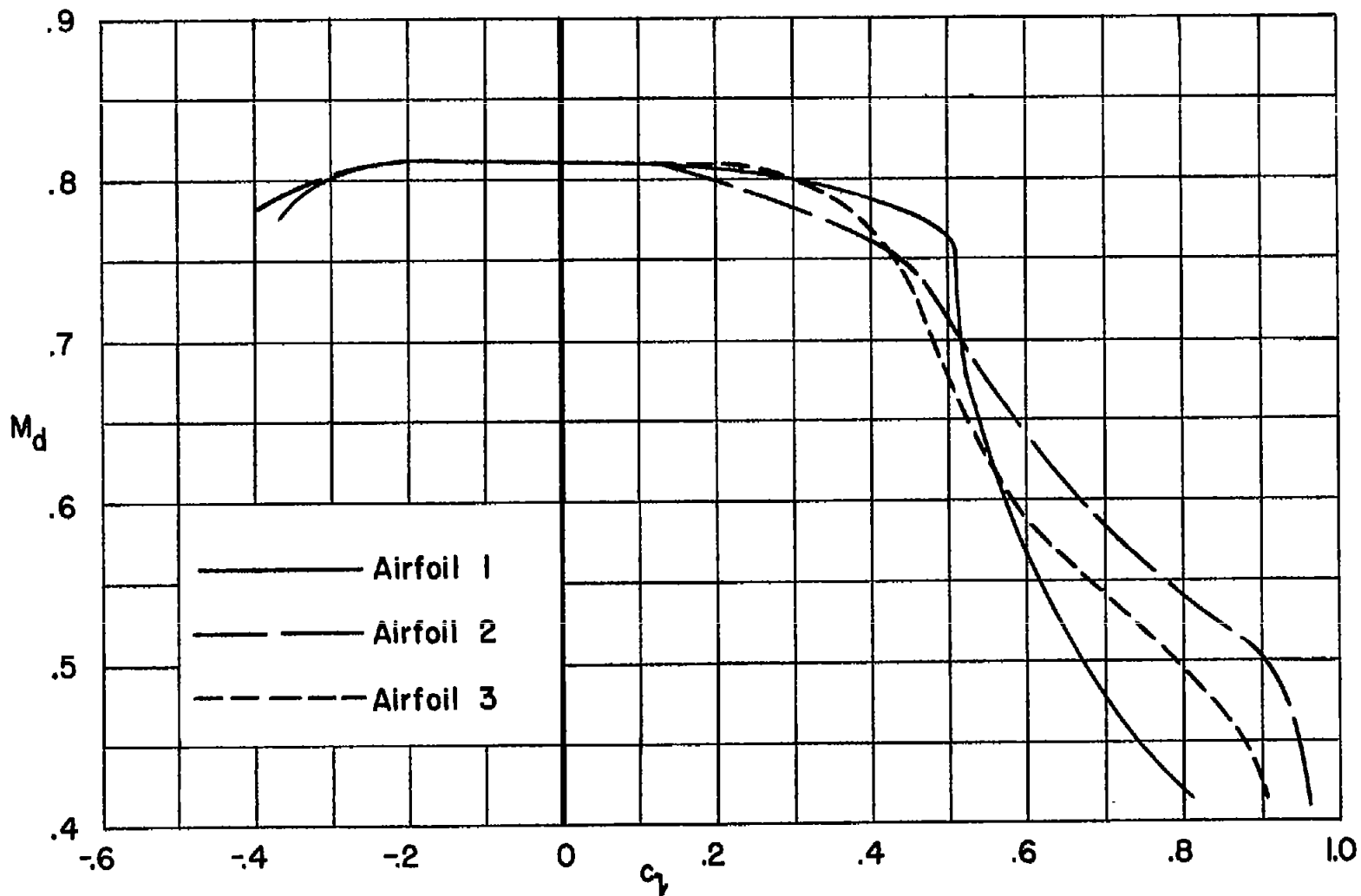


Figure 15.- Comparison of the drag-divergence Mach number characteristics of the modified airfoils.

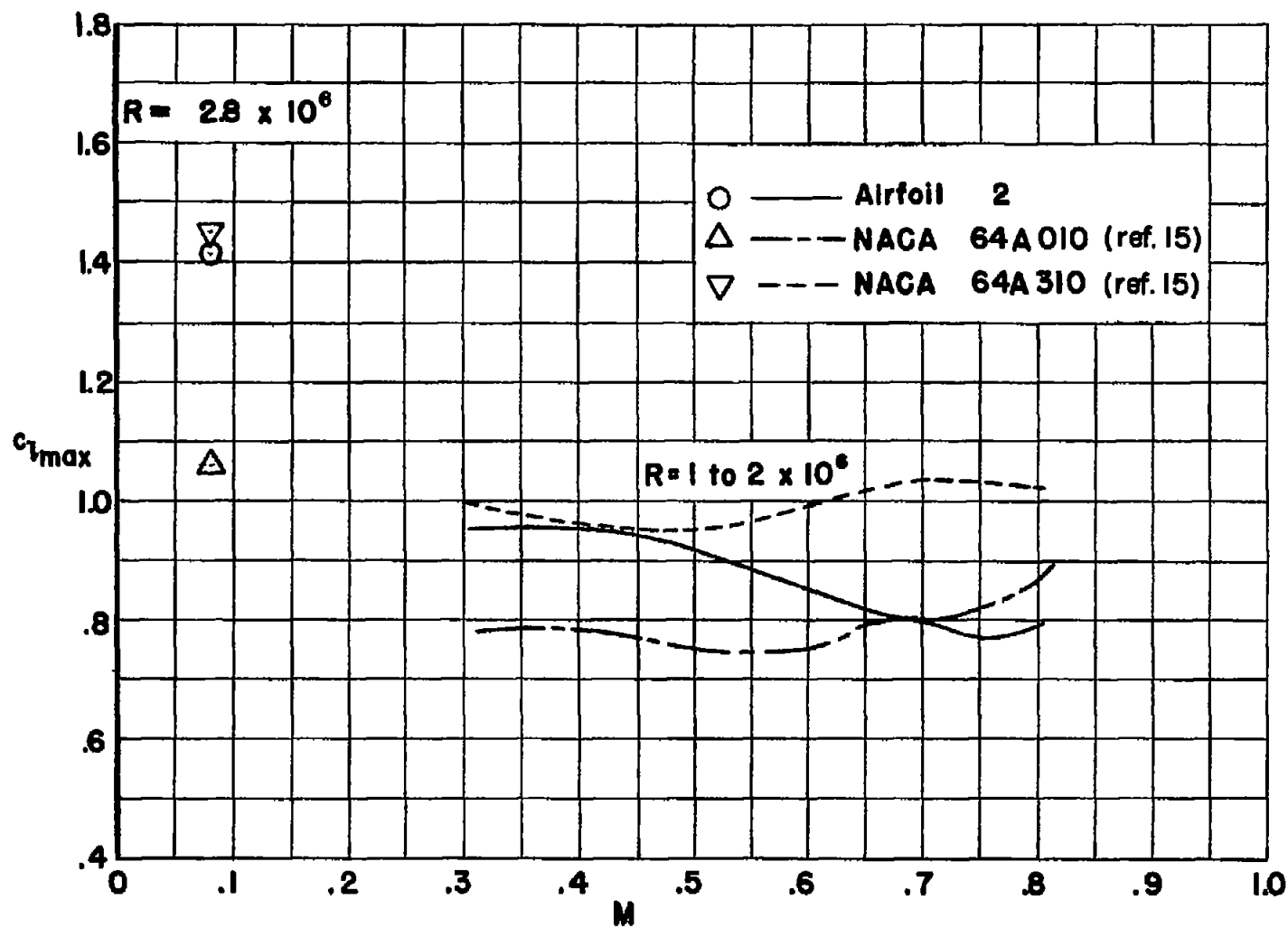


Figure 16.- Variation of $c_{l_{max}}$ with Mach number of airfoil 2, a symmetrical section, and a distributed-camber section.

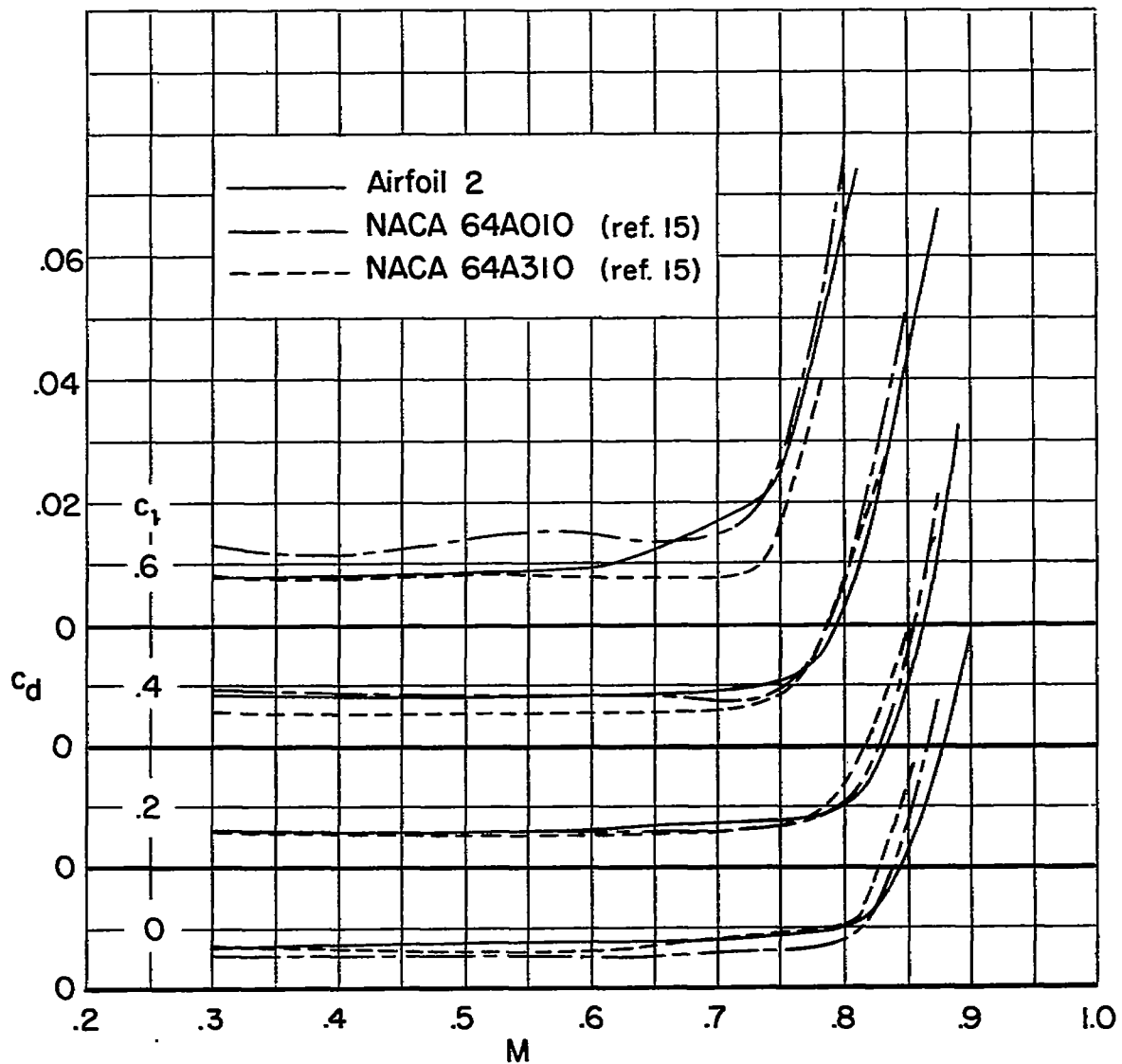


Figure 17.- Comparison of the drag characteristics of airfoil 2, a symmetrical section, and a distributed-camber section.

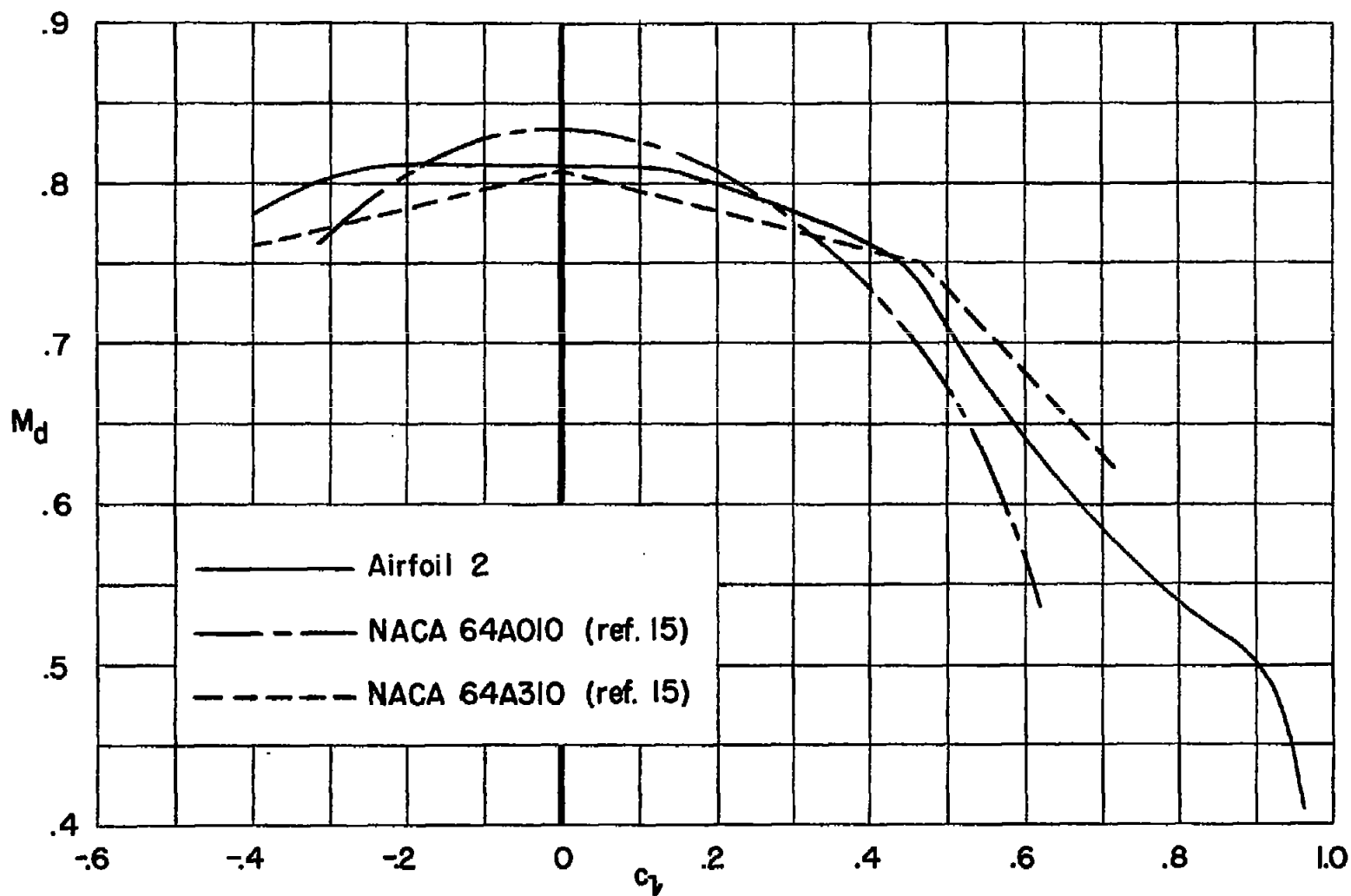


Figure 18.- Comparison of the drag-divergence Mach number characteristics of airfoil 2, a symmetrical section, and a distributed-camber section.

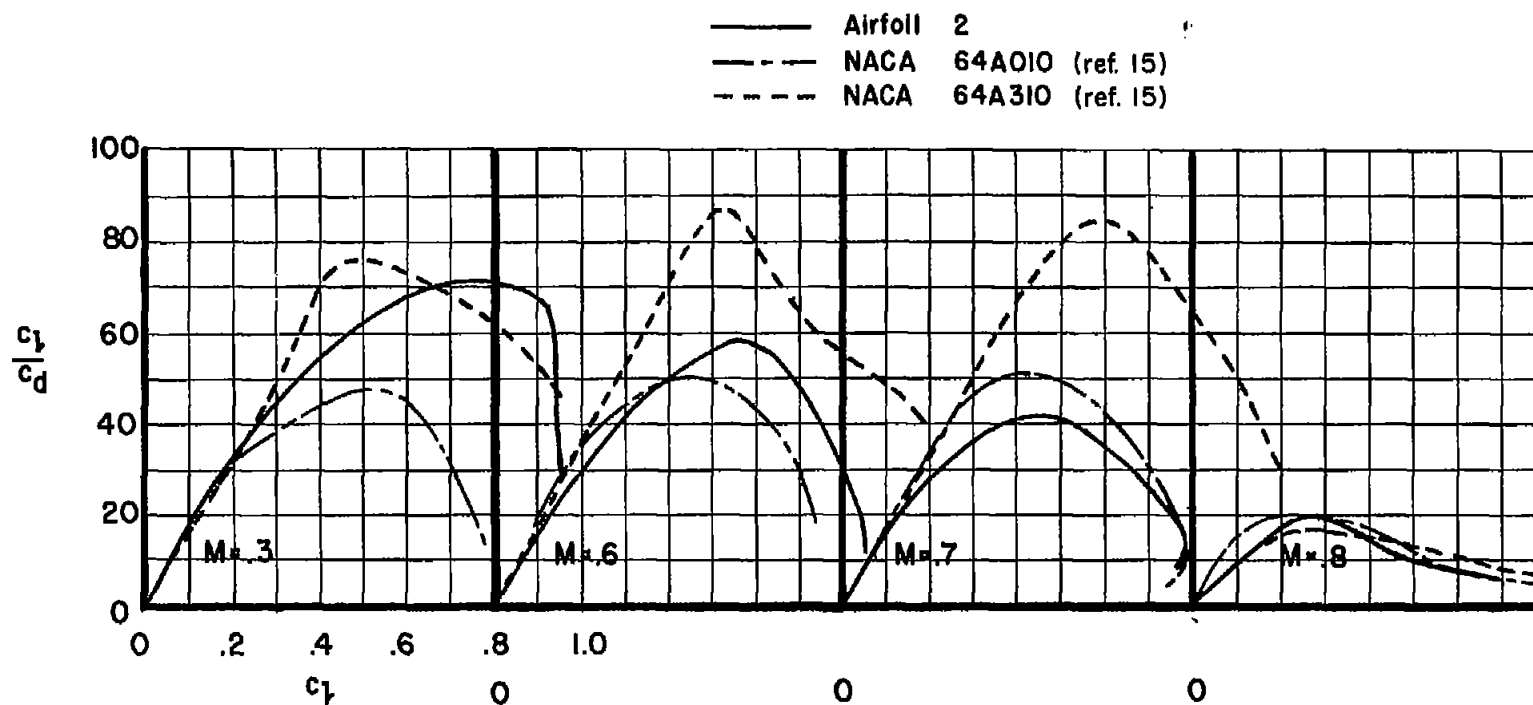


Figure 19.- Lift-drag-ratio characteristics at selected Mach numbers of airfoil 2 and the NACA 64A010 and 64A310 sections.

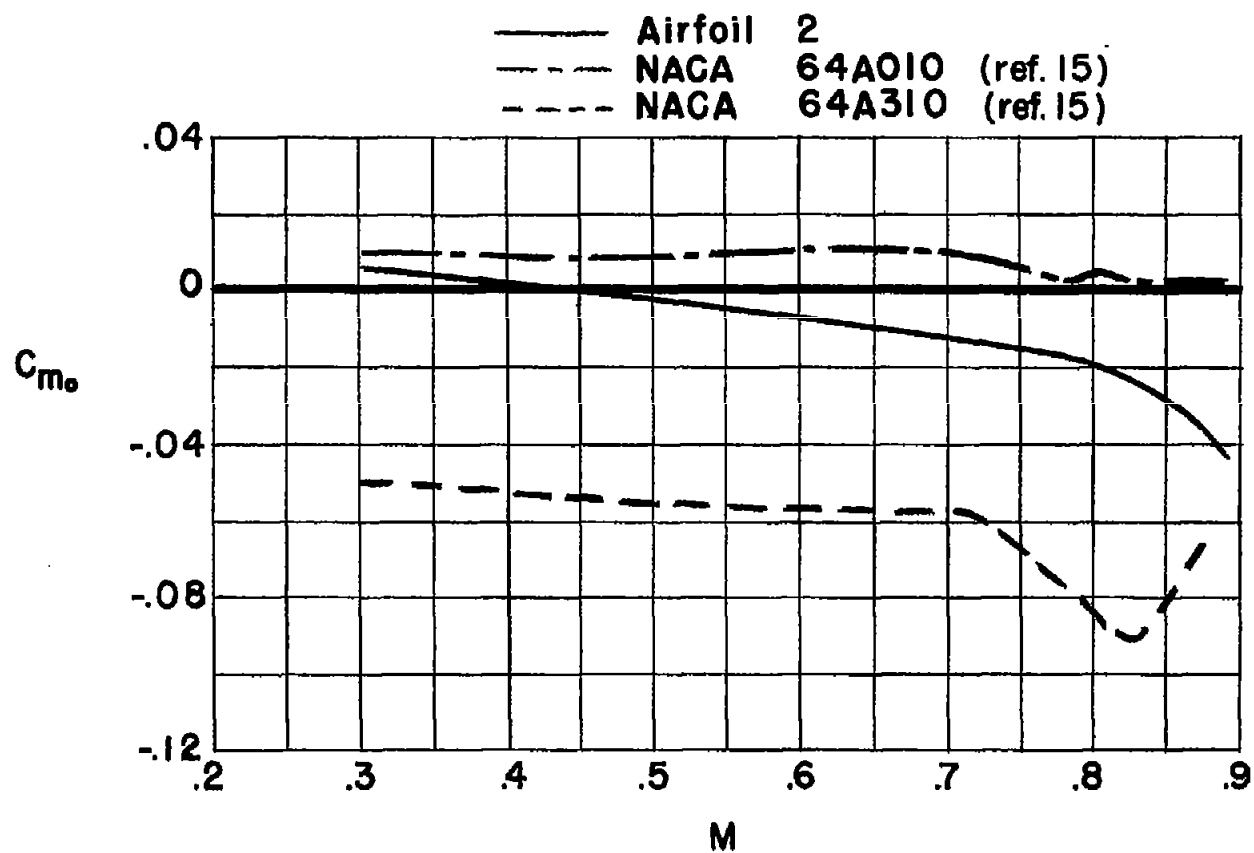


Figure 20.- Variation of zero-lift pitching moment with Mach number of airfoil 2 and the NACA 64A010 and 64A310 sections.